



# Effect on neutrophil migration and antimicrobial functions by the Bruton's tyrosine kinase inhibitors tolebrutinib, evobrutinib, and fenebrutinib

Mirre De Bondt,<sup>1,2,3</sup> Janne Renders,<sup>1</sup> Paloma Petit de Prado,<sup>1</sup> Nele Berghmans,<sup>1</sup> Noémie Pörtner,<sup>1</sup> Lotte Vanbrabant,<sup>1</sup> Vívian Louise Soares de Oliveira,<sup>1</sup> Gayel Duran,<sup>2,3</sup> Paulien Baeten,<sup>2,3</sup> Bieke Broux,<sup>2,3</sup> Mieke Gouwy,<sup>1</sup> Patrick Matthys,<sup>4</sup>  Niels Hellings,<sup>2,3,†</sup> and Sofie Struyf<sup>1,\*</sup> 

<sup>1</sup>Laboratory of Molecular Immunology, Department of Microbiology, Immunology and Transplantation, Rega Institute for Medical Research, KU Leuven, Herestraat 49, 3000 Leuven, Belgium

<sup>2</sup>Neuro Immune Connections & Repair Lab, Department of Immunology and Infection, Biomedical Research Institute, Hasselt University, Agoralaan C, 3500 Hasselt, Belgium

<sup>3</sup>University MS Center, Pelt-Hasselt, Agoralaan gebouw D, 3590 Hasselt, Belgium

<sup>4</sup>Laboratory of Immunobiology, Department of Microbiology, Immunology and Transplantation, Rega Institute for Medical Research, KU Leuven, Herestraat 49, 3000 Leuven, Belgium

\*Corresponding author: Email: [sofie.struyf@kuleuven.be](mailto:sofie.struyf@kuleuven.be)

## Abstract

Multiple sclerosis (MS) is a neurodegenerative, autoimmune disease that is still incurable. Nowadays, a variety of new drugs are being developed to prevent excessive inflammation and halt neurodegeneration. Among these are the inhibitors of Bruton's tyrosine kinase (BTK). Being indispensable for B cells, this enzyme became an appealing therapeutic target for autoimmune diseases. Recognizing the emerging importance of BTK in myeloid cells, we investigated the impact of upcoming BTK inhibitors on neutrophil functions. Although adaptive immunity in MS has been thoroughly studied, unanswered questions about the pathogenesis can be addressed by studying the effects of candidate MS drugs on innate immune cells such as neutrophils, previously overlooked in MS. In this study, we used 3 BTK inhibitors (evobrutinib, fenebrutinib, and tolebrutinib), and found that they reduce neutrophil activation by the bacterial peptide fMLF and the chemokine interleukin-8/CXCL8. Furthermore, they diminished the production of reactive oxygen species and release of neutrophil extracellular traps. Additionally, the production of CXCL8 and interleukin-1 $\beta$  in response to inflammatory stimuli was decreased. Inhibitory effects of the drugs on neutrophil activation were not related to toxicity. Instead, BTK inhibitors prolonged neutrophil survival in an inflammatory environment. Finally, treatment with BTK inhibitors decreased neutrophil migration toward CXCL8 in a Boyden chamber assay but not in a transendothelial setup. Also, in vivo CXCL1-induced migration was unaffected by BTK inhibitors. Collectively, this study provides novel insights into the impact of BTK inhibitors on neutrophil functions, thereby holding important implications for autoimmune or hematological diseases in which BTK is crucial.

**Keywords:** autoimmunity, Bruton's tyrosine kinase signaling, innate immunity, pharmacological inhibitors

## 1. Introduction

Multiple sclerosis (MS) is the most common, immune-mediated, inflammatory disease of the central nervous system (CNS) and is treatable but not curable. Patients are usually diagnosed between the ages of 20 and 40 yr old, with a higher incidence among women than men.<sup>1,2</sup> Despite extensive research, a specific etiologic trigger for MS remains unidentified, but it is evident that it results from a complex interplay between genetic (polymorphisms in HLA class I/II genes) and environmental (smoking, Epstein-Barr virus infection, diet, etc.) risk factors.<sup>3–5</sup> Together, these different factors induce an autoimmune response against different components of the CNS, which manifests through the classical hallmarks of MS: demyelination accompanied by inflammation and neurodegeneration. These damaging processes give rise to the formation of CNS lesions, referred to as sclerotic plaques, which are distributed in both the gray and white matter of the brain.<sup>6</sup> While the

exact pathogenesis of MS remains elusive, it is widely acknowledged that the adaptive immune system plays a central role, with myelin-specific autoreactive T cells as key players. Upon activation, these cells cross the blood-brain barrier (BBB), whereby they encounter CNS-related autoantigens presented by major histocompatibility complex class II molecules on the surface of professional antigen-presenting cells.<sup>7</sup> This triggers the reactivation of T cells, initiating an inflammatory cascade that results in increased production of proinflammatory mediators and the recruitment of other immune cells, causing chronic inflammation and cumulative damage to the CNS. Recent investigations have underscored the significance of the innate immune system, particularly neutrophils, in the onset and development of MS.<sup>8,9</sup> Traditionally perceived as short-lived immune cells, neutrophils are currently also studied in the context of autoimmunity and chronic inflammation.<sup>10</sup> Using both patient samples and animal models for MS, a role for neutrophils in the initiation and progression of the disease has already been highlighted (further reviewed

<sup>†</sup> These authors contributed equally.

**Received:** February 28, 2024. **Revised:** June 14, 2024. **Accepted:** July 4, 2024. **Corrected and Typeset:** July 30, 2024

© The Author(s) 2024. Published by Oxford University Press on behalf of Society for Leukocyte Biology.

This is an Open Access article distributed under the terms of the Creative Commons Attribution License (<https://creativecommons.org/licenses/by/4.0/>), which permits unrestricted reuse, distribution, and reproduction in any medium, provided the original work is properly cited.

in De Bondt et al.).<sup>11</sup> Under normal physiological conditions, neutrophils remain in a quiescent state, surveilling the body without releasing their toxic contents, encapsulated within characteristic granules. During infection or inflammation, these innate immune cells serve as first responders, executing their effector functions upon reaching the site of inflammation. These functions include phagocytosis of micro-organisms, generation of reactive oxygen species (ROS), release of chemokines/cytokines/enzymes, and the formation of neutrophil extracellular traps (NETs), altogether encompassing an excellent mechanism of defense against pathogens.<sup>12</sup> However, these functions may also contribute to chronic inflammation as observed in MS, in which they could be implicated in myelin phagocytosis, disruption of the BBB, activation of antigen-presenting cells, and tissue damage. Currently, various MS drugs with different targets and effector mechanisms are available, all of which slow disease progression without the ability to reverse established damage in the CNS. Among these upcoming treatments for autoimmune diseases, including MS, are the inhibitors of Bruton's tyrosine kinase (BTK).<sup>13</sup>

BTK is a cytoplasmic nonreceptor tyrosine kinase belonging to the TEC kinase family that is expressed in most cells from the hematopoietic lineage, among which neutrophils, as evidenced in the literature and confirmed in our experiments (Supplementary Fig. 1).<sup>14</sup> The activation of BTK occurs through different signaling pathways, dependent on the specific cell type in which it is expressed. It is most widely known for its role in B cell biology, in which BTK acts downstream of the B cell receptor and is crucial for maturation, development, and functioning.<sup>15</sup> Due to its pivotal role in B cell function, BTK is an interesting molecule to target in autoimmune diseases or certain hematological cancers. Ibrutinib, a first-generation BTK inhibitor, is already on the market for treating hematological malignancies.<sup>16</sup> Second-generation compounds (evobrutinib, tolebrutinib, and fenebrutinib) are currently under development for treating MS. These compounds exert their beneficial effect by reducing inflammatory lesions through the inhibition of B cell development, maturation, and functioning, thereby preventing the production of autoantibodies.<sup>17</sup> All inhibitors exhibited promising results in mouse studies using the experimental autoimmune encephalomyelitis model and are currently undergoing phase 3 clinical trials for MS. A dose-dependent reduction in T1 and T2 CNS lesions of patients was observed with all 3 inhibitors in phase 2 clinical trials.<sup>18</sup>

In addition to its established role in B cell biology, BTK was also found to be indispensable for neutrophils. Specifically, Btk-deficient mice display decreased circulating neutrophil numbers, and their neutrophils do not fully mature.<sup>19</sup> However, conflicting data have been reported regarding the impact of BTK on human neutrophil biology.<sup>20,21</sup> Neutrophils isolated from chronic lymphocytic leukemia patients treated with ibrutinib exhibit reduced oxidative burst, degranulation and production of CXCL8 when challenged with *Escherichia coli*.<sup>22</sup> Nevertheless, no published data are available on the influence of second-generation BTK inhibitors on neutrophils. Therefore, this study aimed to unravel the effect of 3 novel inhibitors (fenebrutinib, evobrutinib, and tolebrutinib) on neutrophil effector functions in vitro and in vivo. We demonstrated that treating human neutrophils in vitro with BTK inhibitors (evobrutinib, fenebrutinib, and tolebrutinib) reduces (1) neutrophil activation by CXCL8 or fMLF, (2) migration toward CXCL8 and fMLF in a Boyden chamber assay, (3) ROS production, (4) NET release induced by lipopolysaccharide (LPS), (5) the intralysosomal pH, and (6) the production of CXCL8 and interleukin (IL)-1 $\beta$  by neutrophils. In contrast, migration over a human

endothelial cell monolayer (hCMEC/D3) seemed to be unaffected. Additionally, in vivo migration of mouse neutrophils toward intraperitoneally injected CXCL1 was not disturbed by tolebrutinib. However, the attracted peritoneal neutrophils were less effective in generating ROS. These findings might have important implications for patients' innate immune responses, but can also impact excessive neutrophil activation in chronic inflammatory conditions, such as MS.

## 2. Methods

### 2.1 Reagents

Recombinant human CXCL8(6-77), tumor necrosis factor- $\alpha$  (TNF- $\alpha$ ), interferon- $\gamma$  (IFN- $\gamma$ ), IL-1 $\beta$ , and granulocyte-macrophage colony-stimulating factor were purchased from PeproTech. The bacterial tripeptide fMLF, peptidoglycan (PGN) from *Staphylococcus aureus*, PMA and LPS from *Klebsiella pneumoniae* were purchased from Sigma-Aldrich. Bacterial pHrodo-labeled bioparticles were obtained from Invitrogen. Evobrutinib was purchased from Selleckchem and both fenebrutinib and tolebrutinib from MedChemExpress.

### 2.2 Isolation and treatment of neutrophils

Blood samples from healthy human volunteers were collected in EDTA-coated vacutainer tubes (BD Biosciences) and processed within 15 min after withdrawal. For almost all assays, neutrophils were purified with immunomagnetic isolation using the EasySep direct human neutrophil isolation kit (StemCell Technologies) according to the manufacturer's instructions. For the Boyden chamber migration assay and cytokine induction experiments, neutrophils were purified using density gradient centrifugation, as previously described.<sup>23</sup> Purified neutrophils were subsequently treated for 1 h at 37 °C with the selected inhibitors (evobrutinib, fenebrutinib, and tolebrutinib) all dissolved in treatment medium (1% fetal calf serum [FCS] [Sigma-Aldrich] in phosphate-buffered saline [PBS]).

These concentrations were selected based on a literature survey in which in vitro and in vivo experiments were conducted using comparable concentrations.<sup>21,24–26</sup> Dimethyl sulfoxide (DMSO) (0.01%; Merck) was used as solvent control. After treatment, cell suspensions were centrifuged for 5 min at 300g. Supernatants were discarded and cell pellets were resuspended in the appropriate buffer for the subsequent functional assay. For some assays, another treatment scheme was followed. In that case, the treatment is specifically mentioned in the corresponding paragraph. Independent experiments were performed with cells from different donors, and different donors were used in the different experimental setups. In total, 15 healthy donors were recruited and signed the informed consent (S58418).

### 2.3 Shape change assay

To assess the responsiveness of neutrophils to chemoattractants, shape change assays were performed. CXCL8 (30 ng/mL) or fMLF (10<sup>-9</sup> M) in shape change buffer (Hank's balanced salt solution [HBSS] without Ca<sup>2+</sup> and Mg<sup>2+</sup>, supplemented with 10 mM HEPES; Gibco) was added to a flat-bottom 96-well plate. A buffer-only condition was included as negative control. Isolated neutrophils that were pretreated with BTK inhibitors (see section 2.2) were added to the plate at a concentration of 5 × 10<sup>4</sup> cells/well in prewarmed (37 °C) shape change buffer. After stimulating the cells for 3 min with chemoattractants, neutrophils were fixed with ice-cold 4% (w/v) paraformaldehyde (Thermo Fisher

Scientific) in shape change buffer. A total of 100 cells/well were counted (5 times) microscopically and categorized as either resting/not activated (round) or activated (blebbed and elongated cells). The assessment was performed by 2 independent researchers (MDB, NP), blinded to the experimental setup.

## 2.4 Cytotoxicity assay and cytokine-induced cell death analysis

The toxic effect of the different compounds on freshly isolated neutrophils from healthy donors was assessed through imaging. A sterile 96-well black-walled, flat-bottom plate (Greiner Bio-One) was coated with poly-L-lysine (0.1 mg/mL in sterile water; Sigma-Aldrich) for 1 h at room temperature (RT) to facilitate cellular adhesion. Afterward, the plate was washed twice with sterile distilled water and air-dried in a sterile environment. Neutrophils were purified using immunomagnetic purification (see section 2.2), after which they were washed with medium and mixed with a live/dead staining mix, consisting of EthD-1 (0.5  $\mu$ M, Invitrogen) to stain dead cells and calcein AM (1  $\mu$ M, Invitrogen) to stain live cells. Dead cells (incubated for 15 min at 60 °C) were used as positive control. Medium (Dulbecco's modified Eagle medium FluoroBrite [Gibco] + 0.4% FCS) was used as a negative control. Next,  $5 \times 10^4$  cells/well were seeded in the aforementioned plate, and buffer or different dilutions of the inhibitors (10  $\mu$ M, 1  $\mu$ M or 0.1  $\mu$ M) or diluted solvent (0.1% DMSO) were added. For cytokine-induced cell death analysis, a cytokine mix consisting of TNF- $\alpha$  (50 ng/mL), IL-1 $\beta$  (10 ng/mL), and IFN- $\gamma$  (10 ng/mL) was added after the cells were pretreated for 30 min with inhibitors in the plate. Finally, the plate was inserted into the Incucyte S3 live cell imaging system (Sartorius) and the signal was followed for 5 h (toxicity) or 24 h (survival). Images were processed using Incucyte software where the percentage of dead cells (EthD-1<sup>+</sup>) to total cells (toxicity) or the area under the curve of the number of viable cells (calcein<sup>+</sup>) over time (survival) was calculated.

## 2.5 Oxidative burst assay

To quantify the production of ROS, a chemiluminescence-based assay was performed. Purified neutrophils (human or mouse) were pretreated with BTK inhibitors (10  $\mu$ M–1 nM) or DMSO control (0.01%) for 1 h (see section 2.2). Afterward, cells were washed and suspended in RPMI-1640 medium without phenol red (Gibco) at a final concentration of  $1.5 \times 10^5$  cells/well and added to a white, clear-bottom, 96-well microtiter plate (PerkinElmer). Next, cells were stimulated with the following inducers in the presence of 2 mM luminol (Sigma-Aldrich): PMA (150 ng/mL), TNF- $\alpha$  (10 ng/mL), fMLF ( $10^{-7}$  M for human assay,  $10^{-6}$  M for mouse assay), ultrapure LPS from *K. pneumoniae* (1  $\mu$ g/mL), or PGN from *S. aureus* (1  $\mu$ g/mL). A buffer-only condition was included as control for spontaneous ROS release. Luminol oxidation was measured over time for 3 h at 37 °C using a CLARIOstar monochromator microplate reader (BMG Labtech). Background luminescence (values obtained with PMA stimulation in the absence of luminol) was subtracted and the maximal ROS production was used to calculate the percentage inhibition.

## 2.6 Analysis of NET release

A NETosis assay was performed to quantify the ability of neutrophils to release DNA in response to stimuli, as described previously.<sup>27</sup> Therefore, neutrophils were treated for 1 h with BTK inhibitors or DMSO control (see section 2.2), washed and suspended in colorless RPMI-1640 medium and stained with 50 nM SYTOX Green (Invitrogen). The cells were transferred to a black, clear-bottom

96-well plate ( $5 \times 10^4$  cells/well) that was precoated with poly-L-lysine (see section 2.4), and incubated for 30 min at 37 °C to allow cell adherence. Afterward, LPS from *K. pneumoniae* (1  $\mu$ g/mL), PGN from *S. aureus* (1  $\mu$ g/mL) or PMA (150 ng/mL) were added to the cells and the plate was incubated for 5 h at 37 °C, while NET release was continuously monitored by the Incucyte imaging system. The relative area of SYTOX green fluorescence (DNA released by neutrophils) was determined using the Incucyte S3 software as described and normalized to the number of viable cells.<sup>27</sup>

## 2.7 Phagocytosis analysis

### 2.7.1 Phagocytosis of pHrodo-labeled bioparticles

Uptake of pHrodo-labeled *S. aureus* and *E. coli* bioparticles was investigated (1) microscopically and (2) with flow cytometry. First, a black, clear-bottom 96-well plate was precoated with poly-L-lysine (see section 2.4). Purified neutrophils were pretreated with BTK inhibitors or 0.01% DMSO (see section 2.2), washed and suspended in live cell imaging solution (Invitrogen) supplemented with 20 mM HEPES. Next, cells were stained with calcein AM (1  $\mu$ M) to monitor viability, added to the plate ( $5 \times 10^4$  cells/well), and incubated for 30 min at 37 °C. Afterward, pHrodo bioparticles (62.5  $\mu$ g/mL) were carefully supplemented on top of the cells. Phagocytic uptake of the bioparticles was visualized for 4 h and quantified using the Incucyte imaging system. Second, purified neutrophils were pretreated with BTK inhibitors or 0.01% DMSO (see section 2.2), suspended in buffer (PBS + 2 mM EDTA [Sigma-Aldrich]), and transferred to U-bottom 5 mL tubes ( $5 \times 10^5$  cells/tube). Subsequently, pHrodo *S. aureus/E. coli* bioparticles (625  $\mu$ g/mL) were added to the cells and incubated for 1 h at 37 °C. Afterward, the cells were washed with buffer, centrifuged for 5 min at 300g and the supernatant was discarded. FcR blocking reagent was added (2  $\mu$ L/tube; Miltenyi Biotec) for 15 min, after which the cells were again washed and centrifuged, and the supernatant was discarded. Cells were then stained with anti-CD66b-BV421 (BD Biosciences, #562940) for 25 min at 4 °C in the dark. Cells were washed with staining buffer, centrifuged and the supernatant was discarded. Cell pellets were resuspended in staining buffer and data were acquired with the BD LSR Fortessa X-20 (BD Biosciences) and analyzed with FlowJo software (BD Biosciences; v10.8.1).

### 2.7.2 Phagocytosis of flash red beads

The cells and plates were prepared as described in section 2.7.1. Flash red beads (Bangs Laboratories) were opsonized for 1 h with 20% human serum and added on top of the cells ( $3 \times 10^4$  beads/well). Internalization of the beads was visualized for 4 h and quantified using the Incucyte imaging system. For flow cytometry, opsonized flash red beads ( $3 \times 10^5$  beads/tube) were added to the cells, followed by incubation for 1 h at 37 °C. The subsequent labeling, acquisition and analysis procedure has been described in section 2.7.1.

## 2.8 Cresyl violet staining

To assess the effect of BTK inhibitors on the lysosomal pH of neutrophils, cresyl violet staining was used. Purified neutrophils were pretreated for 1 h with tolebrutinib (1  $\mu$ M) or 0.01% DMSO (see section 2.2). Afterward, the cells were washed with HBSS buffer with Ca<sup>2+</sup> and Mg<sup>2+</sup> (Gibco) and stained for 15 min with cresyl violet (1  $\mu$ M; Sigma-Aldrich). Cells were then washed twice with HBSS buffer and once with flow cytometry buffer (PBS + 2% FCS + 2 mM EDTA) and subsequently divided over U-bottom 5 mL tubes

( $2 \times 10^5$  cells/tube). The subsequent labeling, acquisition, and analysis procedure is described in section 2.7.1.

## 2.9 Boyden chamber assay

A 48-well Boyden chamber chemotaxis assay was performed to measure the chemotactic response of neutrophils toward chemoattractants. Therefore, CXCL8 (30 ng/mL) or fMLF ( $10^{-9}$  M) diluted in Boyden chamber buffer (HBSS buffer with 0.5% human serum albumin [Belgian red cross]) was added to the lower compartment of the Boyden chamber (30  $\mu$ L/well) and subsequently covered with a 5  $\mu$ m pore size polyvinylpyrrolidone-free polycarbonate membrane (GE Water & Process Technologies). A buffer-only condition served as negative control. Neutrophils were pretreated with compounds or control (see section 2.2) and added to the upper part of the chamber ( $1 \times 10^5$  cells/well). Cell migration was allowed for 45 min at 37 °C. Afterward, cells on the membrane were fixed and stained (Hemacolor Solution I-III; Merck). Migrated neutrophils at the lower side of the membrane were microscopically counted in 30 separate fields for each test condition by 2 individual researchers (PPdP, MG) blinded to the experimental setup. The directional migration of the neutrophils toward a chemoattractant is expressed as the chemotactic index. This was calculated by dividing the total number of neutrophils that migrated toward chemoattractant by the total number of cells that migrated toward buffer condition.

## 2.10 In vivo chemotaxis of neutrophils toward CXCL1

### 2.10.1 Mice

Eight-week-old male NMRI mice were purchased from Charles River and housed at the animal facility of the Rega Institute for Medical Research (KU Leuven) in conventional conditions with standards that complied with national and European guidelines. The mice were housed in acrylic filtertop cages (5 mice per cage maximum) and provided with housing enrichment. Water and food were provided ad libitum. All animal studies were approved by the Animal Ethics Committee of KU Leuven (project registry: P114/2022).

### 2.10.2 Chemotaxis of neutrophils toward CXCL1

The mice were weighed and received 0.01% DMSO or tolebrutinib treatment intravenously at a dose of 1 mg/kg (100  $\mu$ L/mouse) diluted in sterile PBS. After an incubation period of 30 min, the mice received an intraperitoneal injection with PBS or recombinant murine CXCL1 (PeproTech; 100 ng/100  $\mu$ L) diluted in PBS. Mice were divided into 4 groups: (1) tolebrutinib treatment and CXCL1 injection, (2) DMSO treatment and CXCL1 injection, (3) tolebrutinib treatment and PBS injection, and (4) DMSO treatment and PBS injection. Chemotaxis of neutrophils was allowed for 2 h after intraperitoneal injections, after which mice were euthanized using dolethal (200 mg/kg, subcutaneous injection; Vetoquinol). The peritoneum was washed for 1 min with 5 mL of PBS supplemented with 2% FCS and 20 U/mL heparin (LEO Pharma).

### 2.10.3 Cytospin analysis

Cytospins were prepared by suspending  $5 \times 10^4$  cells from intraperitoneal lavages in PBS and subsequent centrifugation in a cyto-centrifuge (Shandon) for 8 min at 82.17 *g*, during which the cells were concentrated in a uniform monolayer on a glass slide. After air-drying, the slides were fixed and stained (Hemacolor

solution I-III) and evaluated under a light microscope (50 $\times$  magnification). Each cytospin was counted 3 times ( $3 \times 100$  cells) by 2 individual researchers and the average number of neutrophils as percentage of total cells was calculated.

### 2.10.4 Flow cytometry analysis

For flow cytometry,  $5 \times 10^5$  cells from intraperitoneal lavages were transferred to U-bottom 5 mL tubes and FcR blocking reagent (2  $\mu$ L/tube) and a live/dead stain (Zombie aqua; 1/1,000 dilution in PBS) were added to the tubes. After incubation for 15 min in the dark at RT, the cells were washed with staining buffer (PBS + 2% FCS + 2 mM EDTA) and centrifuged for 5 min at 300 *g*. The supernatant was discarded and the following antibodies were added: anti-CD11b-BUV395 (BD Biosciences; #563553) and anti-Ly6G-PE (BioLegend; #127607). After incubation for 25 min in the dark at 4 °C, the samples were subsequently washed with staining buffer, centrifuged, the supernatant was discarded and the pellet was resuspended in staining buffer. The labeled cells were analyzed with a BD LSR Fortessa. The resulting data were analyzed using FlowJo software.

## 2.11 Immunocytochemistry staining of F-actin and pWASP

Purified neutrophils from healthy donors ( $n = 2$ ) were pretreated for 1 h with tolebrutinib (1  $\mu$ M) or DMSO control (0.01%), after which they were stimulated with fMLF (1  $\mu$ M) for 30 min. Afterward, cells were fixed for 15 min at RT with 4% paraformaldehyde and permeabilized for 10 min at RT with 0.5% Triton-X. After washing with HBSS, cells were incubated with blocking agent (HBSS + 1% bovine serum albumin + 5% goat serum) for 30 min at RT. Afterward, cells were stained overnight with primary rabbit anti-pWASP antibody. Subsequently, a secondary staining mix was added for 1 h at RT, containing Hoechst (10  $\mu$ g/mL; Thermo Fisher Scientific), AF555-Phalloidin (1/400; Thermo Fisher Scientific), WGA-AF647 (1/100; Thermo Fisher Scientific), and goat-anti-rabbit AF488 secondary antibody (1/150; The Jackson Laboratory). Imaging was performed using an Andor Dragonfly High-Speed Confocal Microscope System (Oxford Instruments) at 63 $\times$  magnification. Images were analyzed using ImageJ v1.53c (National Institutes of Health). A representative staining for this assay is shown in [Supplementary Fig. 2](#).

## 2.12 Cell culture

The human cerebral microvascular endothelial cell line hCMEC/D3, provided by Tebu Bio, is a stable and easily cultivatable cell line and the cells display numerous markers of brain endothelial cells, as well as tight and adherens junctions. Cells were cultured in well plates or cell culture T25 and T75 flasks (Greiner Bio-One) after precoating with 75  $\mu$ g/mL collagen type I (0.5% solution from bovine calf skin; MATRIX BioScience) diluted in PBS. After incubation for 1 h at RT, the collagen solution was removed and the coated flasks were rinsed with sterile PBS. hCMEC/D3 cells were cultured in complete endothelial cell growth medium (EGM-2 MV) composed of EBM-2 (Lonza), supplemented with 2.5% FCS, 5 ng/mL vascular endothelial growth factor, 5 ng/mL human epidermal growth factor, 5 ng/mL human basic fibroblast growth factor, 15 ng/mL human insulin-like growth factor-I, 50  $\mu$ g/mL ascorbic acid, 1.4  $\mu$ M hydrocortisone, 10  $\mu$ g/mL gentamycin, and 1  $\mu$ g/mL amphotericin (all from Lonza). For all applications, hCMEC/D3 cells were used at  $\pm 80\%$  confluency between passage 29 and 35 and cultured at 37 °C in a humidified 5% CO<sub>2</sub> incubator.

### 2.13 Transmigration of neutrophils over the hCMEC/D3 layer

In this transmigration assay, the hCMEC/D3 cell line was used as a model for the human BBB. On day zero, endothelial cells ( $8.25 \times 10^3$  cells/well) were seeded on ThinCerts ( $3.0 \mu\text{m}$  pore size; translucent; Greiner Bio-One) in a 24-well plate (Greiner Bio-One) suspended in EGM-2 MV medium. On days 3 and 5, the inserts were replenished with experimental medium (EBM2+), composed of EBM-2 medium supplemented with 1 ng/mL human basic fibroblast growth factor, 1.4  $\mu\text{M}$  hydrocortisone, 10  $\mu\text{g}/\text{mL}$  gentamicin, 1  $\mu\text{g}/\text{mL}$  amphotericin, and 2.5% FCS. On day 7, the hCMEC/D3 cells were treated with inflammatory cytokines TNF- $\alpha$  (100 ng/mL) and IFN- $\gamma$  (10 ng/mL) in serum reduced experimental medium (EBM2+ SR-HC), consisting of EBM-2 medium supplemented with the same factors as experimental EBM2+ medium, but with only 0.25% FCS and without hydrocortisone. After 4 h of inflammation, medium was discarded and cells were washed with EBM2+ SR-HC medium to remove the inflammatory cytokines. Purified neutrophils were pretreated with BTK inhibitors or DMSO as described in section 2.2 (diluted in EBM2+ SR-HC medium) and were labeled with 1  $\mu\text{M}$  calcein AM for 30 min at 37 °C. In the bottom compartment of the wells, 10 ng/mL CXCL8 or regular EBM2+ SR-HC medium was added. Stained neutrophils were added ( $5 \times 10^5$  cells/insert) and migration was allowed for 2 h at 37 °C, after which both the upper and lower compartment suspensions were collected and calcein fluorescence was measured in a CLARIOstar reader (BMG LABTECH).

### 2.14 Neutrophil inductions for cytokine and chemokine quantification

Neutrophils were induced for 24 h with different stimuli in the presence of BTK inhibitors to measure chemokine/cytokine production. First,  $5 \times 10^5$  cells/well were suspended in medium (RPMI-1640 with phenol red + 10% FCS + 50  $\mu\text{g}/\text{mL}$  gentamycin [Gibco] + 5 ng/mL granulocyte-macrophage colony-stimulating factor) and added to a flat-bottom 48-well plate. Subsequently, the cells were pretreated for 1 h at 37 °C with different dilutions of BTK inhibitors and controls (0.01% DMSO and medium only). After treatment, the cells were incubated for 24 h at 37 °C, 5% CO<sub>2</sub>, in the presence of different inducers: LPS from *K. pneumoniae* (1  $\mu\text{g}/\text{mL}$ ), fMLF ( $10^{-6}$  M), TNF- $\alpha$  (priming 10 min, 50 ng/mL) + IL-1 $\beta$  (100 ng/mL), or TNF- $\alpha$  (priming 10 min, 50 ng/mL) + IFN- $\gamma$  (100 ng/mL). Afterward, the well content was collected and centrifuged for 5 min at 300 *g*. Finally, the supernatants were stored at -20 °C for further analysis. The concentration of CXCL8 was measured by an in-house developed sandwich enzyme-linked immunosorbent assay (ELISA).<sup>28</sup> The concentration of IL-1 $\beta$  was determined using the human IL-1 $\beta$ /IL-1F2 DuoSet ELISA kit (DY201-05; Bio-Techne; R&D Systems), according to the manufacturer's protocol. Absorbance was measured at 450 nm by using a PowerWave XS (BioTek) microplate reader.

### 2.15 Statistics

Raw data from the different functional assays are shown as percentage inhibition, i.e. the outcome value of BTK inhibitor-treated neutrophils compared with that of the DMSO control-treated neutrophils (0% inhibition = experimental outcomes are the same for inhibitor and control neutrophils; 100% inhibition = outcome of inhibitor-treated neutrophils is reduced to zero as compared with control-treated neutrophils). The normality of the data was first evaluated using a Shapiro-Wilk test and subsequently corresponding downstream statistical testing was applied with a

correction for multiple testing. The applied statistical tests are indicated in the figure legends. Statistical analysis and visualization of the data were performed using GraphPad Prism 9.3.1 (GraphPad Software).

### 2.16 Ethics approval

All procedures performed in studies involving human participants were in accordance with the ethical standards of the institutional and/or national research committee and with the 1964 Helsinki Declaration and its later amendments or comparable ethical standards. The study was approved by the Ethics Committee of the University Hospital Leuven (study number: S58418). All animal studies were approved by the Animal Ethics Committee of KU Leuven (project registry: P114/2022).

### 2.17 Consent to participate

All human participants donating peripheral blood for neutrophil isolation signed an informed consent form according to the ethical guidelines of the Declaration of Helsinki (study number: S58418).

## 3. Results

### 3.1 Treatment with BTK inhibitors significantly reduces the activation of neutrophils by CXCL8 and fMLF

The first step in a neutrophil's response to a chemoattractant is activation of the cytoskeleton and a concurrent shape change, from round to blebbed or even elongated. To assess the effect of BTK inhibitors on neutrophil activation by fMLF and CXCL8, purified neutrophils from healthy donors were treated for 1 h with 1 or 10  $\mu\text{M}$  inhibitor, after which the cells were stimulated with CXCL8 or fMLF for 3 min. To evaluate the effect of the inhibitors on activation, neutrophils were microscopically scored as resting cells (round, Fig. 1A) or activated cells (blebbed/elongated, Fig. 1B) and the percentage activated cells of total cells was calculated. Next, the percentage inhibition by the different compounds, compared with solvent control (DMSO), was calculated. Almost all tested concentrations of BTK inhibitors inhibited neutrophil activation significantly by both fMLF (Fig. 1C) and CXCL8 (Fig. 1D). To further unravel the responsible pathway for this effect, we quantified total F-actin content and phosphorylation of the downstream signaling molecule WASP. Using confocal microscopy, we detected a significant reduction in the F-actin and pWASP signal after fMLF stimulation in tolebrutinib-treated neutrophils, compared with DMSO control (Fig. 1E, F).

### 3.2 BTK inhibitors are not cytotoxic and protect neutrophils from cytokine-induced cell death

To exclude the possibility that the compounds interfered with neutrophil activation by inducing cell death, a toxicity assay was performed. After treatment with different concentrations of BTK inhibitors, cells were stained with calcein AM and EthD-1 to stain viable and dead cells, respectively. For 5 h, the percentage of dead cells among the total cells was calculated every 30 min. No toxicity was detected for any of the tested concentrations of compound or solvent control (Fig. 2A). When a cytokine mix (TNF- $\alpha$ , IL-1 $\beta$ , and IFN- $\gamma$ ) was added to the cells to mimic inflammation, prolonged viability (followed for 24 h) was observed for neutrophils that were pretreated with BTK inhibitors compared

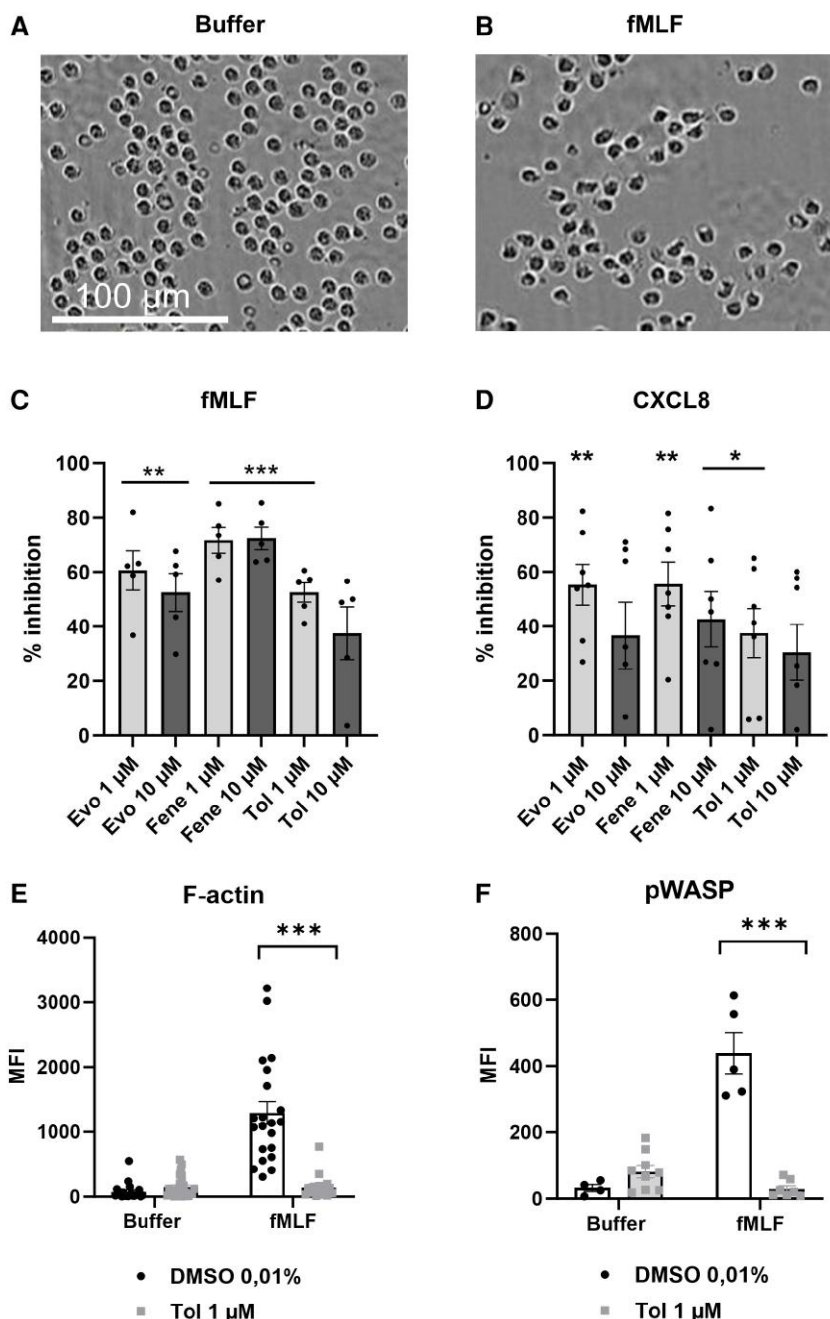


**Fig. 1.** All BTK inhibitors reduce neutrophil activation by fMLF and CXCL8. (A, B) Representative image of DMSO-treated neutrophils stimulated with (A) buffer or (B) 1 nM fMLF. Purified neutrophils from healthy donors ( $n = 5$  to 7) were pretreated for 1 h with (C, D) BTK inhibitors (evobrutinib, fenebrutinib, and tolebrutinib) at concentrations of 1  $\mu$ M or 10  $\mu$ M or solvent control (0.01% DMSO). Afterward, neutrophils were activated with (C) fMLF (1 nM) or (D) CXCL8 (30 ng/mL) for 3 min. Cells were then fixed and microscopically scored as resting (round) or activated (blebbed/elongated) and the percentage activated cells of total cells was calculated. Next, the percentage inhibition of the treatments compared with DMSO control was calculated from the percentage activation. Normally distributed data are represented as the mean  $\pm$  SEM and statistically analyzed using a 1-sided t test with Bonferroni correction: \* $P < 0.05$ , \*\* $P < 0.01$ , \*\*\* $P < 0.001$  (% inhibition by the BTK inhibitors is different from 0). (E, F) Purified neutrophils from healthy donors ( $n = 2$ ) were pretreated for 1 h with tolebrutinib (1  $\mu$ M) or DMSO control (0.01%), after which they were stimulated with fMLF (1  $\mu$ M) for 30 min. Cells were imaged with a confocal microscope at 63 $\times$  magnification. Median fluorescence intensity (MFI) of pWASP and F-actin signal was quantified with ImageJ for 10 cells per image, and each dot represents the result of 1 image. Normally distributed data are shown as mean  $\pm$  SEM and analyzed with an unpaired t test. \*\*\* $P < 0.001$ .

with DMSO or buffer control (Fig. 2B). Under control conditions, neutrophils started dying after approximately 7 h of incubation in RPMI-1640 medium (Fig. 2C). However, after stimulation with cytokines, DMSO-treated cells started dying after 4 h. In contrast, cytokine-induced cell death was delayed up to 10 h upon treatment with BTK inhibitors (Fig. 2C).

### 3.3 BTK inhibitors interfere with the release of spontaneous and stimulus-induced ROS

The release of ROS comprises one of the most powerful effector mechanisms of neutrophils against pathogens, especially bacteria and fungi.<sup>29</sup> Activating stimuli such as fMLF and TNF- $\alpha$  have been shown to be highly potent inducers of ROS production by

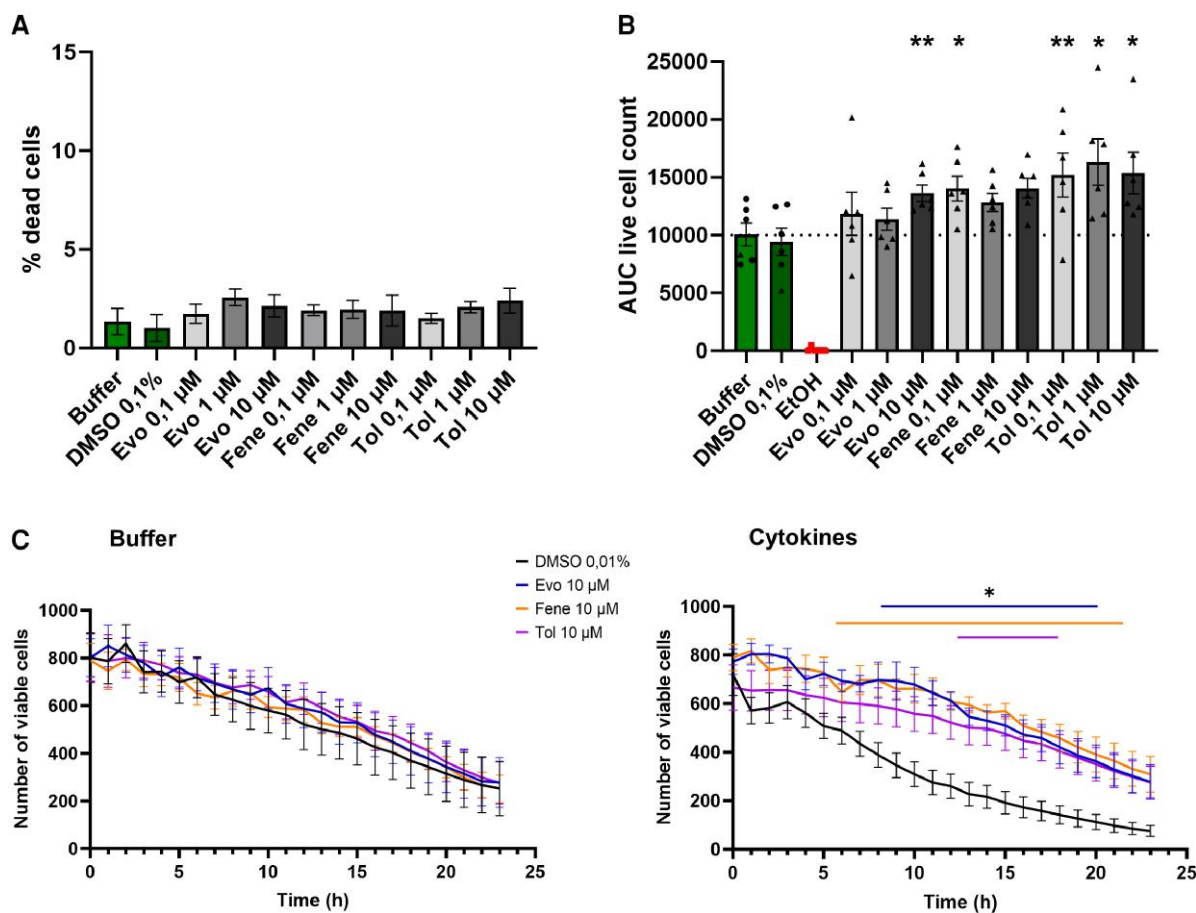


**Fig. 2.** None of the compounds induces neutrophil toxicity, but BTK inhibitors increase cell viability after cytokine stimulation. (A) Purified neutrophils from healthy donors ( $n = 6$ ) were treated with BTK inhibitors (evobrutinib, fenebrutinib, or tolebrutinib) at concentrations of 0.1  $\mu\text{M}$ , 1  $\mu\text{M}$ , or 10  $\mu\text{M}$ . Calcein AM (1  $\mu\text{M}$ ) and EthD-1 (0.5  $\mu\text{M}$ ) were added to visualize live and dead cells, respectively. DMSO (0.1%) and buffer were used as vehicle and negative control. The cells were imaged for 5 hours in the Incucyte imaging system and the percentage of dead cells (EthD-1+) was calculated. Data are represented as the median  $\pm$  IQR and statistically analyzed using a nonparametric 1-way analysis of variance with Dunn's correction. (B, C) Purified neutrophils from healthy blood samples ( $n = 6$ ) were stained with calcein AM (1  $\mu\text{M}$ ) and pretreated for 30 min with BTK inhibitors (0.1  $\mu\text{M}$ , 1  $\mu\text{M}$ , or 10  $\mu\text{M}$ ). Afterward, cells were stimulated with a cytokine mixture, composed of IFN- $\gamma$  (10 ng/mL), TNF- $\alpha$  (50 ng/mL), and IL-1 $\beta$  (10 ng/mL). Viability was quantified over time using the Incucyte imaging system, and (B) the area under the curve (AUC) was calculated when (C) monitoring the number of viable cells. Data are represented as the mean  $\pm$  SEM and statistically analyzed using (B) a Friedman test with Dunn's correction or (C) 2-way analysis of variance with Šidák correction. \* $P < 0.05$ , \*\* $P < 0.01$ .

neutrophils in vitro.<sup>30</sup> To assess whether the selected BTK inhibitors affect ROS release, purified neutrophils from healthy donors were pretreated with the compounds for 1 h and stimulated with either buffer, to study spontaneous ROS release, or one of the inducers (fMLF, TNF- $\alpha$ , PGN, LPS, or PMA). Afterward, ROS production was quantified by a chemiluminescence assay (Fig. 3A-E and Supplementary Fig. 3A-E), and for each drug, the percentage inhibition compared with solvent control was calculated.

Surprisingly, spontaneous ROS release was already completely inhibited after treatment with BTK inhibitors (Fig. 3A). Next, we evaluated ROS production after stimulation with PMA, which serves as a positive control, as PMA directly activates protein kinase C (PKC) and subsequent ROS production without receptor involvement. After stimulation with PMA, no difference in ROS production was detected in BTK inhibitor-treated conditions compared with controls, indicating that the ROS machinery is still functional (Fig. 3B, E). In response to TNF- $\alpha$  or fMLF stimulation, strong inhibition on ROS production was observed after treatment with all 3 BTK inhibitors (Fig. 3C, D). A similar effect was obtained following LPS and PGN activation, and a dose-dependent

inhibition could be observed (Fig. 3E). Finally, the effect of tolebrutinib (1  $\mu\text{M}$ ) on LPS-induced mitochondrial ROS production was also investigated, which again resulted in a reduction of the maximal ROS production, compared with DMSO control (Supplementary Fig. 3F).

### 3.4 Treatment with BTK inhibitors decreases the release of NETs after stimulation with LPS but not with PGN

Another neutrophilic microbicidal effector function is the release of NETs, which are fiber-like structures of DNA that trap and eliminate pathogens. NETs are composed of decondensed chromatin, associated with different neutrophil antimicrobial proteins, released during a process called NETosis.<sup>31</sup> As ROS production is crucial for the formation of NETs, we sought to investigate the effect of BTK inhibitors on NET release. Some known inducers that stimulate NET release are PMA, which activates the PKC pathway, and components of the bacterial cell wall, such as LPS, present in gram-negative bacteria, and PGN, present in both gram-positive and negative bacteria.<sup>32</sup> To study

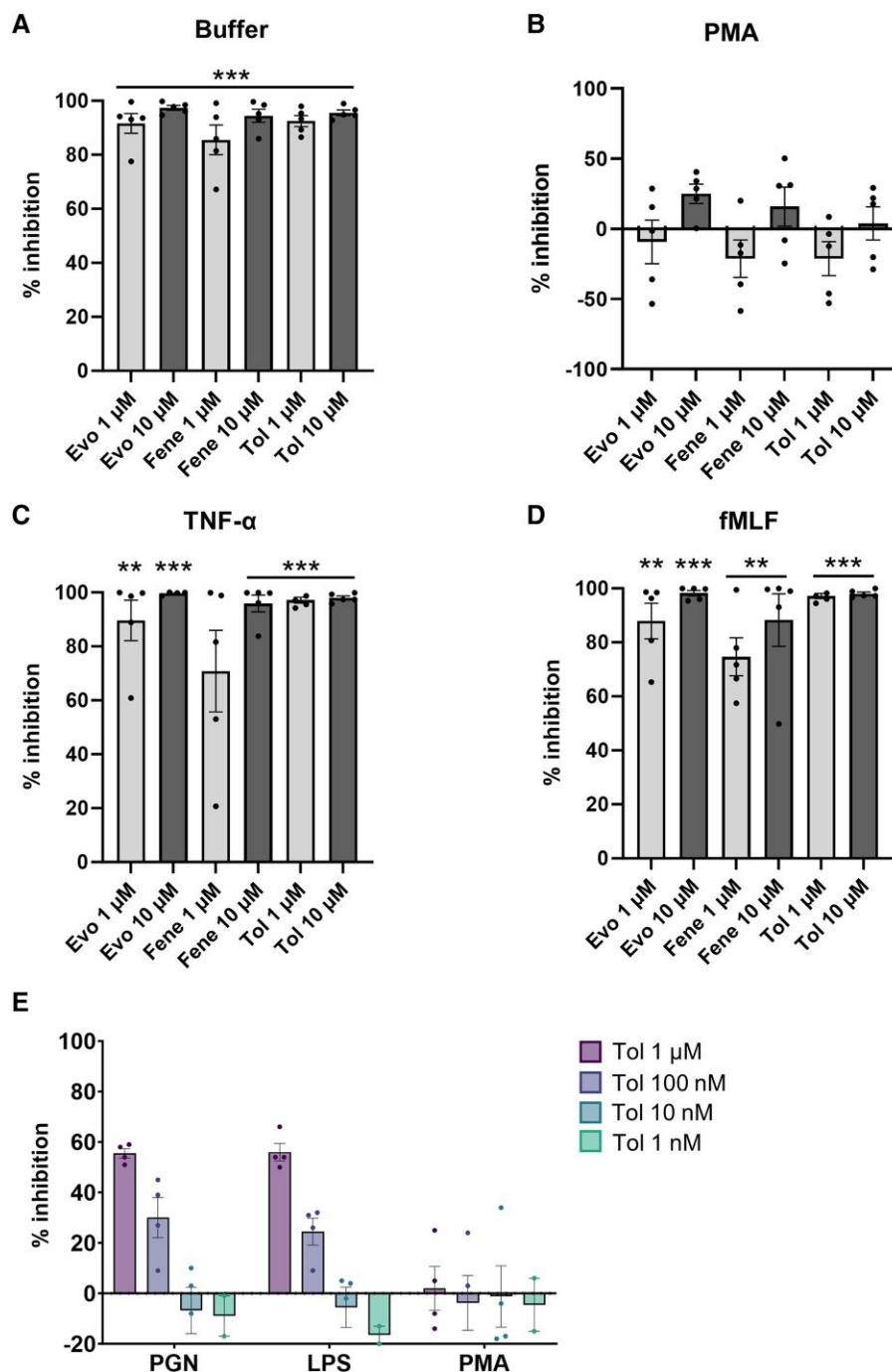


**Fig. 3.** Spontaneous and stimulus-evoked ROS production is almost completely inhibited after treatment with BTK inhibitors, in a dose-dependent manner. Purified neutrophils from healthy donors ( $n = 4$  to  $5$ ) were pretreated for 1 h with BTK inhibitors (evobrutinib, fenebrutinib, or tolebrutinib) at concentrations of  $10 \mu\text{M}$ – $1 \text{nM}$  or with  $0.01\%$  DMSO control. Afterward, neutrophils were stimulated with inducers, and luminol ( $2 \text{mM}$ ) was added to quantify ROS release via luminescence. The following inducers were used (A) buffer, as a measure for spontaneous ROS release; (B, E) PMA ( $150 \text{ng/mL}$ ), as positive control; (C) TNF- $\alpha$  ( $10 \text{ng/mL}$ ); (D) fMLF ( $0.1 \mu\text{M}$ ); (E) LPS from *K. pneumoniae* ( $1 \mu\text{g/mL}$ ); or (E) PGN from *S. aureus* ( $1 \mu\text{g/mL}$ ). The percentage inhibition by BTK inhibitors compared with solvent control ( $0.01\%$  DMSO) is shown. Normally distributed data are represented as the mean  $\pm$  SEM and were statistically analyzed using a 1-sided t test with Bonferroni correction: \*\* $P < 0.01$ , \*\*\* $P < 0.001$  (% inhibition by the BTK inhibitors is different from 0).

the effect of BTK inhibitors on NET release over time, purified neutrophils from healthy donors were pretreated with BTK inhibitors and stimulated with PMA, LPS, or PGN. The released NETs were then visualized using SYTOX green and quantified using the Incucyte imaging system (Fig. 4A). The area of NETs after 5 h was normalized to the cell area at time point 0. Afterward, the effect of each compound on NET secretion was calculated

as the percentage inhibition relative to the solvent control. Our results show that upon stimulation with LPS, treatment with evobrutinib and tolebrutinib significantly reduced the release of NETs compared with DMSO control (Fig. 4B). On the other hand, after stimulation with PGN or PMA, no effect on NET production was detected after treatment with BTK inhibitors (Supplementary Fig. 4).



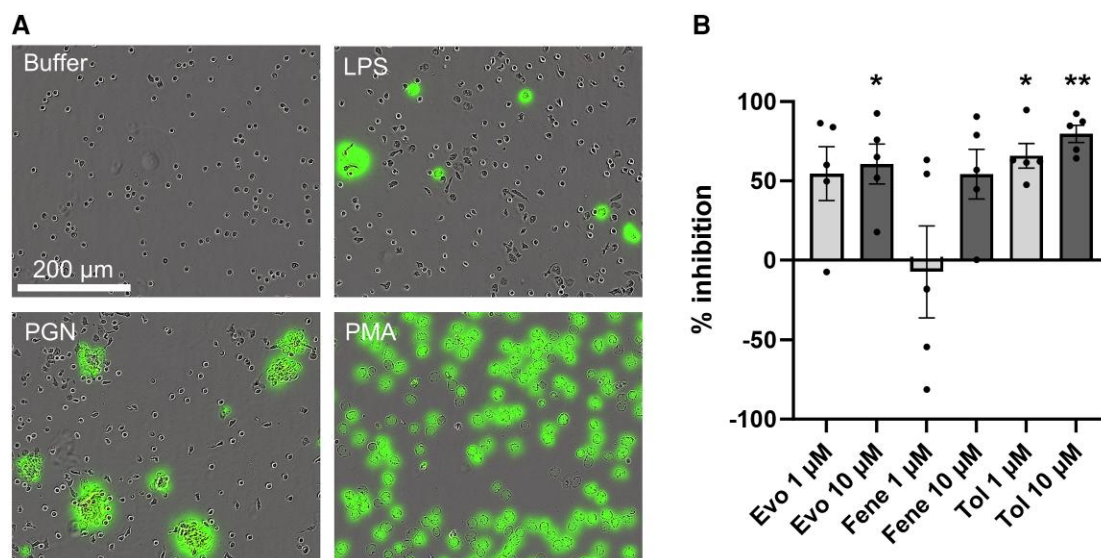


**Fig. 4.** LPS release of neutrophil extracellular traps is reduced by BTK inhibitors. (A) Representative Incucyte image showing NETs released by untreated (i.e. no BTK inhibitors present) neutrophils after 4 h of incubation with buffer, LPS from *K. pneumoniae* (1 μg/mL), PGN from *S. aureus* (1 μg/mL), or PMA (150 ng/mL). (B) Purified neutrophils from healthy donors ( $n = 5$ ) were pretreated for 1 h with 0.01% DMSO as control or BTK inhibitors (evobrutinib, fenebrutinib, or tolebrutinib) at concentrations of 1 μM or 10 μM. Afterward, neutrophils were stimulated with LPS in the presence of SYTOX green (0.5 mM) to visualize extracellular DNA release in the Incucyte system. The area of NETs after 5 hours of stimulation was normalized to the cell area at  $T = 0$ . The percentage inhibition on NET release (after 5 h) of the inhibitors compared with solvent control (0.01% DMSO) was calculated. Data are represented as the mean  $\pm$  SEM and were statistically analyzed using a 1-sided t test with Bonferroni correction: \* $P < 0.05$ , \*\* $P < 0.01$  (% inhibition by the BTK inhibitors is different from 0).

### 3.5 Phagolysosomes are more acidic after treatment with BTK inhibitors

Neutrophils also exert their microbicidal function by ingesting pathogens and eliminating them through the release of ROS or antimicrobial peptides and enzymes into the phagolysosome. To evaluate the effect of the selected treatments on bacterial phagocytosis over time, purified neutrophils from healthy donors were pretreated with BTK inhibitors for 1 h. Subsequently, their phagocytic capacity was stimulated using pH-sensitive *S. aureus* or *E. coli* bioparticles. These particles will only emit a red fluorescent signal upon uptake in an acidic environment, such as the phagolysosome of a neutrophil, which can be detected in the Incucyte imaging system or via flow cytometry. For Incucyte analysis, *S. aureus* or *E. coli* bioparticles were added to neutrophils that were pretreated with BTK inhibitors and stained with calcein. The obtained intracellular red fluorescence intensity (red fluorescence colocalizing with green fluorescence, Fig. 5A) 4 h after the addition of stimulus was normalized to the area of live neutrophils at time point 0. Surprisingly, we observed an enhanced signal for *S. aureus* bioparticles in neutrophils treated with BTK inhibitors, compared with buffer or DMSO control, which was significant at a dose of 1 μM tolebrutinib (Fig. 5B). To ensure that this was not a bacterial-specific effect, we repeated the experiment with *E. coli* bioparticles and again found the same significant increase in tolebrutinib-treated neutrophils, compared with DMSO control (Fig. 5C). Next, we wanted to confirm these results using flow cytometry. Treating neutrophils with tolebrutinib again resulted in an increased red fluorescence intensity of the phagocytosing neutrophils, for both *S. aureus* and *E. coli* (Supplementary Fig. 5A). However, the percentage of neutrophils that internalized a bioparticle was not affected after treatment with tolebrutinib (Fig. 5D). We next incubated neutrophils with flash red beads, which are Toll-like receptor (TLR) ligand-free fluorescent microspheres that are not pH sensitive. When repeating the experiments with

flash red beads instead of pH sensitive, bacterial bioparticles, we found no effect of tolebrutinib treatment on the percentage of neutrophils that internalized a bead using either flow cytometry (Supplementary Fig. 5B) or the Incucyte (Supplementary Fig. 5C) for analysis. This led us to hypothesize that the inhibition of BTK does not affect the phagocytosis machinery, but rather influences the acidity of the phagolysosomes, as the fluorescence intensity of the bioparticles is proportional to the lysosomal pH. We explored this hypothesis by staining neutrophils that were pretreated with tolebrutinib or DMSO with cresyl violet, a fluorescent pH indicator.<sup>33</sup> Confirming our hypothesis, we found an increased cresyl violet signal for neutrophils that were treated with tolebrutinib compared with DMSO control (Fig. 5E), indicative for a lower lysosomal pH in the BTK inhibitor-treated neutrophils.

### 3.6 BTK inhibitors decrease in vitro neutrophil migration

For neutrophils to fight pathogens or resolve inflammation, they need to be able to reach the site of infection/inflammation. Recognition of activating stimuli will thereby cause circulating neutrophils to migrate toward the site of injury, guided by a chemical gradient, a process better known as chemotaxis. To investigate whether migration of neutrophils is also affected by BTK inhibitors, we studied neutrophil chemotaxis toward CXCL8 and fMLF. Cells were therefore treated for 1 h with compounds or DMSO control, after which the migration was assessed using a Boyden chamber migration assay (Fig. 6 and Supplementary Fig. 6). First, we ensured that none of the inhibitors affected the spontaneous migration of neutrophils toward buffer (data not shown). Furthermore, we found that tolebrutinib and evobrutinib at 10 μM were able to significantly inhibit neutrophil migration toward CXCL8, whereas fenebrutinib significantly reduced migration toward fMLF (Fig. 6A). To ensure that the effect of BTK inhibition on neutrophil migration could not be attributed to a change in

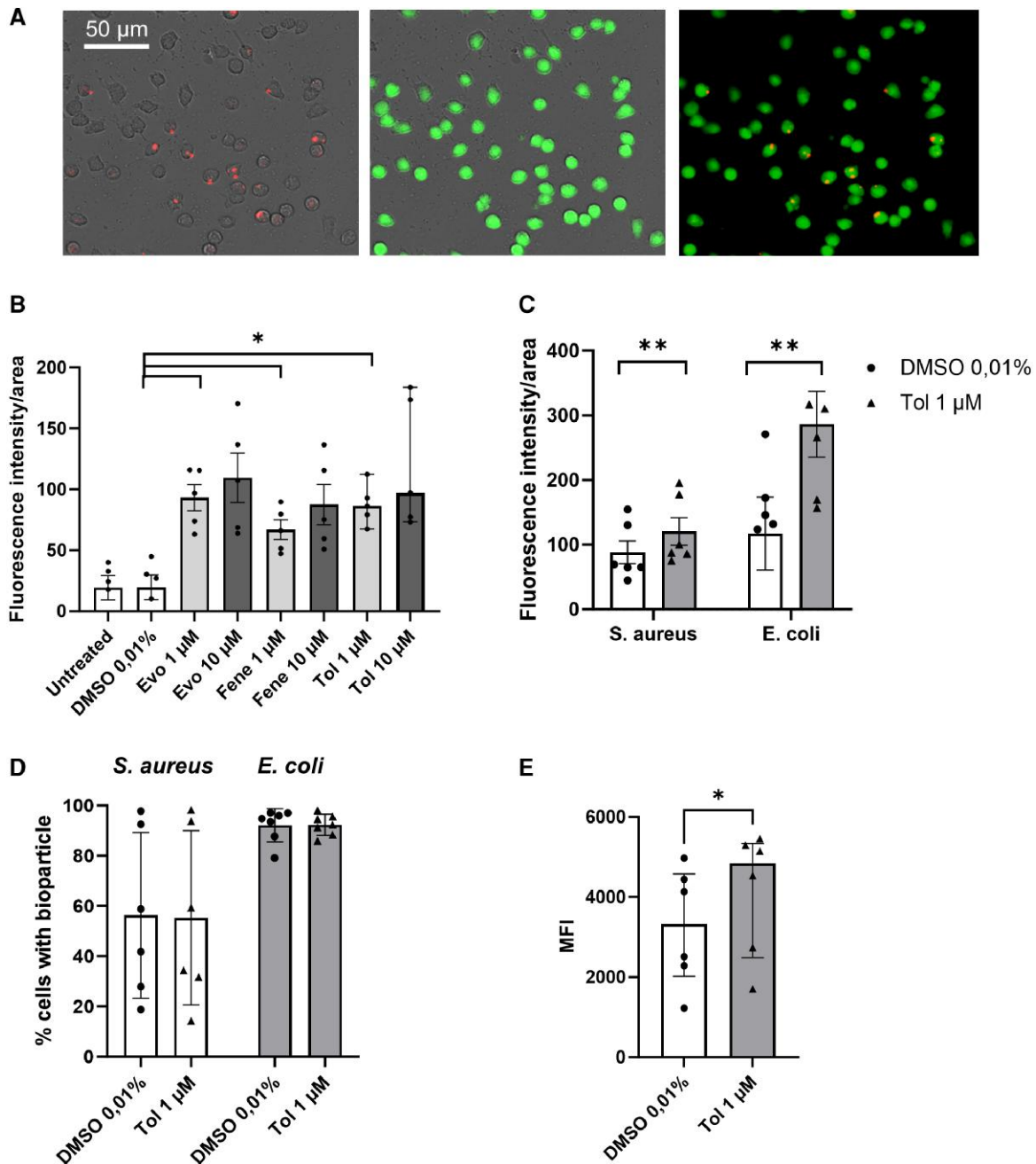


**Fig. 5.** Treatment of neutrophils with BTK inhibitors does not affect phagocytosis but makes lysosomes more acidic. (A) Representative Incucyte image of internalized beads (red) in live, control neutrophils (green) after 4 h,  $\times 20$  objective. Purified neutrophils from healthy donors were pretreated for 1 h with BTK inhibitors (evobrutinib, fenebrutinib, and tolebrutinib) at concentrations of 1  $\mu\text{M}$  or 10  $\mu\text{M}$  or 0.01% DMSO and buffer as vehicle and untreated control. (B, C) Neutrophils from different donors ( $n = 5$ ) were stained with calcein AM (1  $\mu\text{M}$ ) for 30 min and pHrodo *S. aureus* or *E. coli* bioparticles (62.5  $\mu\text{g}/\text{mL}$ ) were added. Phagocytosis was imaged for 4 h with the Incucyte system. The fluorescent intensity of the bioparticles (red) after 4 h was normalized to the live cell area (green) at time point 0. Data are represented as the mean  $\pm$  SEM and were statistically analyzed using (B) 1-way analysis of variance with Dunnett's correction or (C) paired t test: \* $P < 0.05$ , \*\* $P < 0.01$ . (D) Neutrophils from different donors ( $n = 6$ ) were incubated for 1 hour with pHrodo *S. aureus* or *E. coli* bioparticles and then stained with anti-CD66b antibody. Cells were analyzed using the BD LSR Fortessa, and data are represented as percentage neutrophils (CD66b+) positive for pHrodo signal. Data are represented as mean  $\pm$  SEM and analyzed with a paired t test. (E) Neutrophils from different donors ( $n = 6$ ) were incubated with cresyl violet (1  $\mu\text{M}$ ) for 15 min. Cells were analyzed with the BD LSR Fortessa, and the median fluorescence intensity (MFI) of the dye in gated CD66b+ cells was calculated with FlowJo. Data are represented as median  $\pm$  IQR and were analyzed using a Wilcoxon paired t test: \* $P < 0.05$ .

the expression of the surface receptors for CXCL8 and fMLF, we quantified the expression level of the receptors by flow cytometry. After treating the neutrophils for 1 h with tolebrutinib, we evaluated the expression of CXCR1, CXCR2, and FPR1. We found no changes in median fluorescence intensity of any of the receptors upon BTK inhibitor treatment (Supplementary Fig. 7).

### 3.7 In vivo chemotaxis of neutrophils toward CXCL1 is not influenced by treatment with BTK inhibitors, but ROS production is reduced

Next, the effect of BTK inhibitors on neutrophil chemotaxis was further explored in vivo. Healthy mice were intravenously injected with DMSO (0.5%) or tolebrutinib (1 mg/kg). After this,

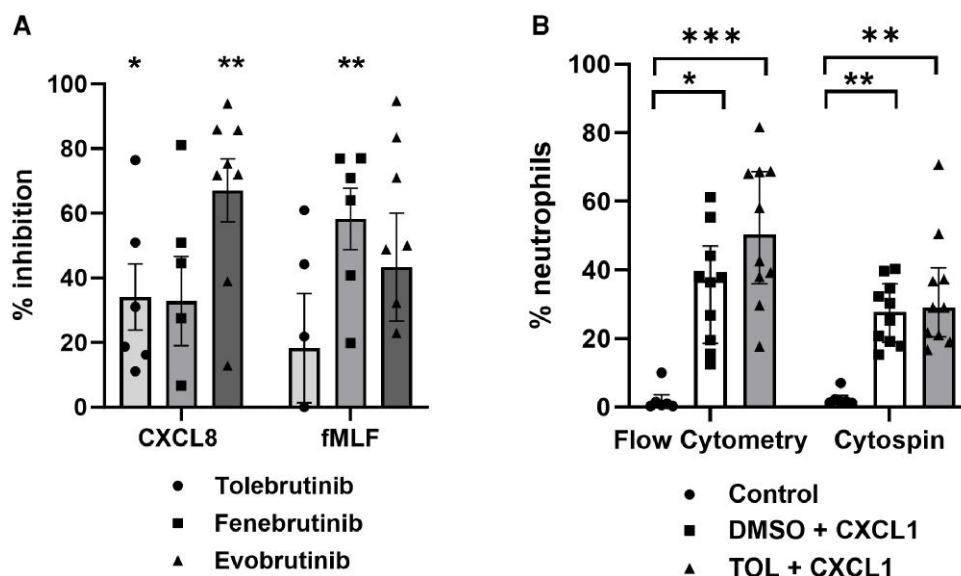


**Fig. 6.** In vitro migration of neutrophils toward CXCL8 and fMLF is reduced by BTK inhibitors, whereas in vivo migration to CXCL1 is not affected. (A) Purified neutrophils from healthy donors ( $n = 4$  to  $8$ ) were pretreated for 1 h with BTK inhibitors (evobrutinib, fenebrutinib, and tolebrutinib) at  $10 \mu\text{M}$  or 0.01% DMSO control. Afterward, neutrophils were added to the upper compartment of a Boyden chamber, containing CXCL8 ( $10 \text{ ng/mL}$ ) or fMLF ( $1 \text{ nM}$ ) in the lower wells. The reduction in chemotactic index (i.e. the number of migrated cells toward stimulus divided by the number of migrated cells toward buffer) of the treatment groups compared with solvent control (0.01% DMSO) was calculated and expressed as percentage inhibition. Data are represented as the mean  $\pm$  SEM and were statistically analyzed using a 1-sided  $t$  test with Bonferroni correction: \* $P < 0.05$ , \*\* $P < 0.01$  (% inhibition by the BTK inhibitors is different from 0). (B) NMRI mice received an intravenous injection of 0.5% DMSO ( $n = 13$ ) or tolebrutinib ( $n = 13$ ;  $1 \text{ mg/kg}$ ). After 30 min, the mice were injected intraperitoneally with PBS ( $n = 6$ ) or recombinant murine CXCL1 ( $1 \text{ ng}/\mu\text{L}$ ;  $n = 20$ ). Two hours after intraperitoneal injections, the percentage neutrophils in the intraperitoneal lavages were determined via flow cytometry analysis or by microscopic analysis of cytospin preparations. Data are presented as median  $\pm$  IQR and were statistically analyzed using a nonparametric 1-way analysis of variance with Dunn's correction: \* $P < 0.05$ , \*\* $P < 0.01$ , \*\*\* $P < 0.001$ .

chemotaxis of neutrophils was induced by intraperitoneal injection of CXCL1, a potent mouse neutrophil chemoattractant often used to mimic CXCL8-induced effects in humans, as CXCL8 does not exist in mice. After 2 h, the percentage of neutrophils in the peritoneal lavage was determined via 2 independent techniques that delivered similar results. Peritoneal lavages were analyzed with flow cytometry, in which cells double positive for CD11b and Ly6G were identified as neutrophils. Additionally, neutrophils were microscopically counted via classical cytospin analysis. Both analyses indicated that significantly more neutrophils were recruited toward the peritoneum when CXCL1 was injected in DMSO-treated mice compared with the PBS control (Fig. 6B). However, a similar increased percentage of neutrophils attracted by CXCL1 was detected in the tolebrutinib-treated mice. Moreover, the total number of neutrophils and total cells in the peritoneal lavages were not affected by tolebrutinib (data not shown). Therefore, in contrast to the results from the Boyden chamber assay, in vivo neutrophil chemotaxis in response to CXCL1 does not seem to be affected by tolebrutinib treatment.

As BTK inhibitors were previously used in mice, predominantly to study B cell activity, we wanted to ensure that tolebrutinib was able to affect mouse neutrophils at all. To this end, we purified mouse neutrophils from the bone marrow of control mice and performed an in vitro ROS chemiluminescence assay. Using different stimuli, we confirmed our results obtained with human neutrophils. After pretreatment of mouse neutrophils with tolebrutinib, evobrutinib, or DMSO control, we found that spontaneous ROS production (buffer) as well as LPS- or fMLF-induced ROS release was reduced by BTK inhibitors compared with solvent control (Supplementary Fig. 8A–D). As PMA-induced ROS production was not affected by treatment with BTK inhibitors, we confirmed that the ROS machinery was still intact after

pretreatment. These data exclude the possibility that BTK inhibitors are not able to affect mouse neutrophils. To ensure that the intravenously injected tolebrutinib in our in vivo setting reached the circulating neutrophils, we performed a final experiment in which we quantified ROS production of the neutrophils attracted to the peritoneum after intraperitoneal injection of CXCL1 in mice that received intravenously DMSO or tolebrutinib. Again, no effect of tolebrutinib on neutrophil migration toward CXCL1 was detected, confirming our earlier findings. However, peritoneal neutrophils from the tolebrutinib-treated mice produced significantly less ROS (Supplementary Fig. 8E). Taken together, our in vivo data show that treating mice intravenously with tolebrutinib does not affect the chemotaxis of neutrophils toward CXCL1. However, the cells that are attracted to the peritoneum were found to have a reduced capacity to produce ROS.

### 3.8 Neutrophil migration over an endothelial barrier is increased toward CXCL8 and after inflammation but is unaffected by tolebrutinib or evobrutinib

Following up on the conflicting findings from the Boyden chamber assay and the in vivo chemotaxis experiment, we wanted to assess in vitro neutrophil migration in a more physiological context. When neutrophils are attracted toward the site of inflammation, they need to transmigrate from the circulation into the affected tissue, thereby crossing an endothelial barrier. To simulate this, a transmigration assay was performed in which neutrophils migrate over inserts covered with a uniform monolayer of endothelial cells. Neutrophils were pretreated with BTK inhibitors or DMSO control and stained with calcein. Afterward, they were added on top of the hCMEC/D3-covered inserts, and the

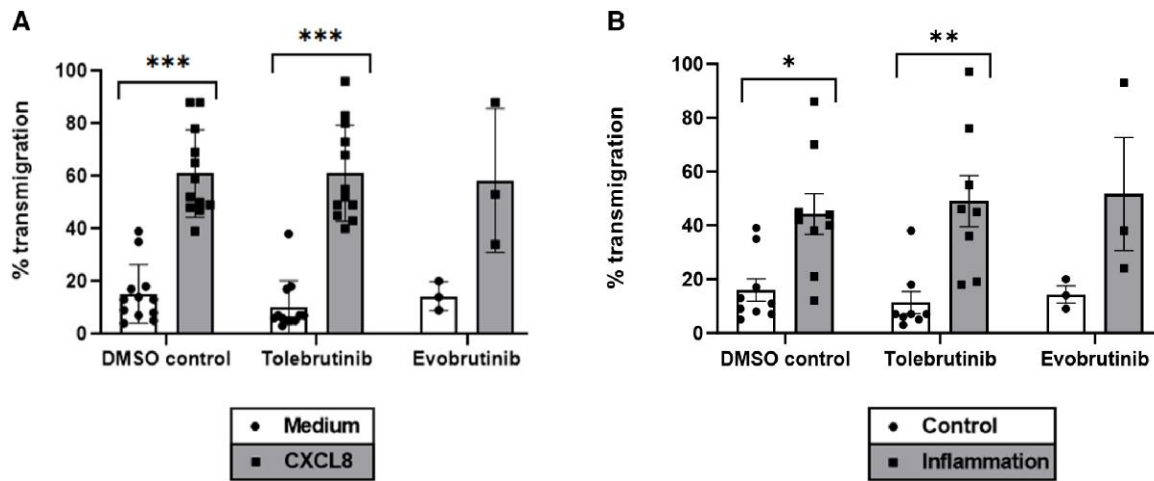


**Fig. 7.** Neutrophil migration over an in vitro BBB model is increased toward CXCL8 and after inflammation of the endothelium. Purified neutrophils from healthy donors ( $n = 3$  to  $12$ ) were stained with calcein AM ( $1 \mu\text{M}$ ) and afterward treated for 1 h with DMSO ( $0.01\%$ ) as vehicle control, or with the BTK inhibitors tolebrutinib and evobrutinib ( $10 \mu\text{M}$ ). The neutrophils were added to the upper compartment of the endothelium-covered inserts and migrated over the hCMEC/D3 cells for 2 h. Results are shown as percentage transmigration, i.e. the fluorescence in the lower compartment relative to the total fluorescence (sum of the measured fluorescence in the upper and lower compartment after incubation). (A) Neutrophils migrated toward serum reduced experimental medium or CXCL8 ( $10 \text{ ng/mL}$ ) after treatment with DMSO ( $n = 12$ ), tolebrutinib ( $n = 12$ ) or evobrutinib ( $n = 3$ ). (B) Neutrophils migrated over a normal or inflamed endothelium toward medium. Inflammation of the endothelium was induced by treatment with TNF- $\alpha$  ( $100 \text{ ng/mL}$ ) and IFN- $\gamma$  ( $10 \text{ ng/mL}$ ) for 4 hours prior to addition of neutrophils. Data are presented as the mean  $\pm$  SEM and were statistically analyzed using a 2-way analysis of variance with Sidák correction: \* $P < 0.05$ , \*\* $P < 0.01$ , \*\*\* $P < 0.001$ .

percentage of transmigration (i.e. the fluorescence signal at the bottom divided by the fluorescence signal at the top + bottom) after 2 h was calculated for each condition. The results indicated that migration toward CXCL8 was significantly increased compared with migration toward medium, in all the treatment groups (Fig. 7A). The same trend was observed with endothelium treated with TNF- $\alpha$  and IFN- $\gamma$ , i.e. a significant increase in transmigration by both the DMSO- and tolebrutinib-treated cells (Fig. 7B). In contradiction with the results of the Boyden chamber assay, but in line with our in vivo data, no significant effect of BTK inhibitor treatment on CXCL8-induced migration of neutrophils was detected, and BTK inhibitors did not influence migration over an inflamed endothelial layer. A kinetics experiment was conducted to compare 1, 2, and 4 h of transendothelial migration, but all time points resulted in the same migration percentages irrespective of the BTK inhibitor treatment (data not shown).

### 3.9 The production of CXCL8 and IL-1 $\beta$ by neutrophils is reduced after treatment with BTK inhibitors

In response to activating stimuli, neutrophils are able to produce and release different molecules (e.g. the chemokine CXCL8 and the cytokine IL-1 $\beta$ ) that function as mediators of the immune response by enhancing the activation and recruitment of immune cells, including neutrophils, to the site of inflammation.<sup>34</sup> To study the effect of BTK inhibitors on release of CXCL8 and IL-1 $\beta$ , purified neutrophils from healthy donors were incubated for 24 h in the presence of different inducers. Afterward, the level of CXCL8 and IL-1 $\beta$  in the supernatants was determined using a sandwich ELISA (Fig. 8 and Supplementary Fig. 9), and the percentage inhibition compared with solvent control ( $0.01\%$  DMSO) was calculated. Regarding CXCL8, our results already suggest a reduced baseline CXCL8 production in the BTK inhibitor-treated groups relative to control (Fig. 8A). Furthermore, CXCL8 production stimulated by the bacterial peptide fMLF was significantly reduced by all tested BTK inhibitors (Fig. 8B). CXCL8 production in

response to treatment with LPS from *K. pneumoniae* was strongly inhibited after treatment with all BTK inhibitors (Fig. 8C). Finally, when CXCL8 release was induced by a combination of the cytokines TNF- $\alpha$  and IL-1 $\beta$ , a significant decrease was detected in the treatment groups (Fig. 8D). IL-1 $\beta$  production, induced by LPS from *K. pneumoniae*, was significantly lower after treatment with some BTK inhibitors (Fig. 8E). Last, IL-1 $\beta$  release in response to TNF- $\alpha$  and IFN- $\gamma$  was significantly decreased in most of the treatment groups (Fig. 8F).

## 4. Discussion

In this study, we explored the impact of a novel class of disease-modifying therapies for the treatment of MS on neutrophil functions. Specifically, we focused on the emerging BTK inhibitors, currently undergoing phase 3 clinical trials for MS. The role of the BTK enzyme in neutrophil biology has recently gained attention, yet conclusive data on its impact on neutrophil effector functions remain lacking.<sup>19,26,35–39</sup> Neutrophils are the first responding cells of the innate immune system that combat pathogens and react to inflammatory cues. In chronic inflammatory conditions, these functions can become pathogenic and contribute to inflammation and tissue damage. Consequently, studying the effects of therapeutic compounds on neutrophils is essential, as these compounds may influence patients' immune responses. Moreover, such studies contribute to our understanding of the mechanism of action of these compounds.

To confirm the inhibitory capacity in neutrophils, we first quantified the activation of BTK through the phosphorylation of tyrosine 223 following fMLF activation. We detected a significant reduction in pBTK levels after tolebrutinib treatment, compared with control, which confirms the functionality of the inhibitors (Supplementary Fig. 1).

Our findings indicate that all BTK inhibitors, namely evobrutinib, fenebrutinib, and tolebrutinib, strongly influenced neutrophil functionality. In a shape change assay, we observed a notable

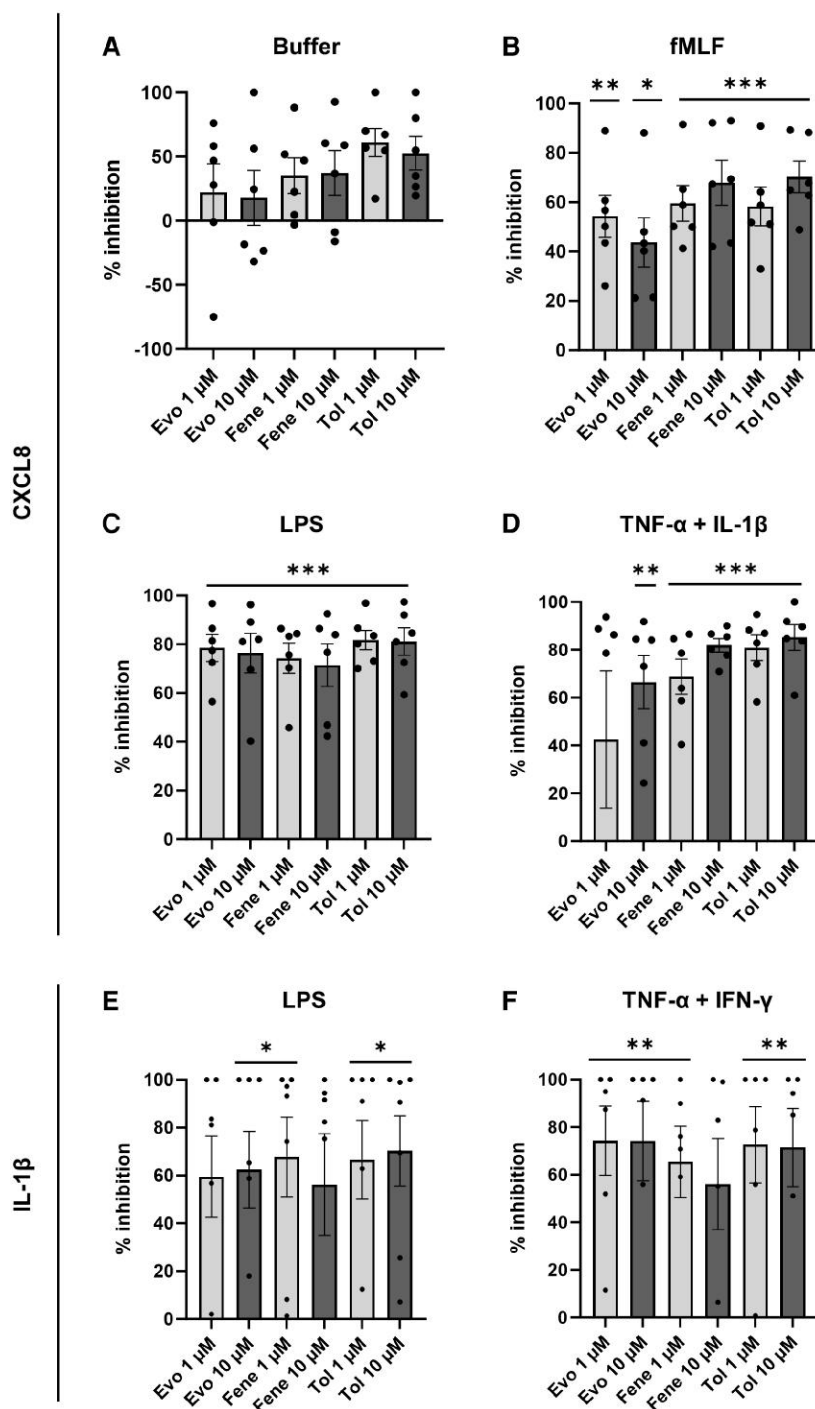


**Fig. 8.** The production of CXCL8 and IL-1 $\beta$  by neutrophils is reduced after treatment with BTK inhibitors. Purified neutrophils from healthy donors ( $n = 5$  to 6) were pretreated for 1 h with BTK inhibitors (evobrutinib, fenebrutinib, and tolebrutinib) at concentrations of 1 or 10  $\mu\text{M}$  or 0.01% DMSO control. Afterward, neutrophils were stimulated for 24 h with different inducers, and CXCL8 (A–D) or IL-1 $\beta$  (E, F) production was quantified by ELISA. The percentage inhibition by BTK inhibitors on CXCL8 or IL-1 $\beta$  release compared with solvent control (0.01% DMSO) was calculated. Cells were treated with (A) medium only (background production), (B) fMLF (1  $\mu\text{M}$ ), (C, E) LPS from *K. pneumoniae* (1  $\mu\text{g}/\text{mL}$ ), (D) TNF- $\alpha$  (priming for 10 min; 50 ng/mL) in combination with IL-1 $\beta$  (100 ng/mL), and (F) TNF- $\alpha$  (priming for 10 min; 50 ng/mL) in combination with IFN- $\gamma$  (100 ng/mL). Data are represented as the mean  $\pm$  SEM and were statistically analyzed using a 1-sided t test with Bonferroni correction: \* $P < 0.05$ , \*\* $P < 0.01$ , \*\*\* $P < 0.001$  (% inhibition by the BTK inhibitors is different from 0).

reduction in neutrophil activation by both CXCL8 and fMLF with all 3 compounds. Cellular activation involves cytoskeleton remodeling, particularly actin polymerization, which was described to be BTK dependent through the activation of the signaling protein WASP.<sup>40</sup> Following on this, our results confirmed a significant reduction in the total F-actin levels and the phosphorylation

(Tyr290) of WASP upon tolebrutinib pretreatment. This is consistent with the results reported by Herter et al.<sup>41</sup> indicating a decrease in fMLF-induced phosphorylation of BTK and reduced MAC-1 activation following pretreatment with PRN473, a specific BTK inhibitor, both in vitro and in vivo. Remarkably, we noted an extended lifespan of neutrophils stimulated with cytokines

(TNF- $\alpha$ , IFN- $\gamma$ , and IL-1 $\beta$ ) after pretreatment with BTK inhibitors. Given that BTK directly interacts with NLRP3, ASC, and procaspase 1 for inflammasome activation and IL-1 $\beta$  signaling, BTK inhibition can reduce inflammasome-induced pyroptosis in murine neutrophils and macrophages.<sup>42</sup> Furthermore, pretreatment of neutrophils with BTK inhibitors strongly inhibited both spontaneous and stimulus-evoked ROS production by human and murine neutrophils, in a dose-dependent manner. This aligns with literature suggesting that BTK is involved in pathways leading to NADPH oxidase assembly and myeloperoxidase release, critical for the formation of oxygen reactants. FPR1 occupation by fMLF induces G protein-mediated activation of phosphoinositide 3-kinase and phospholipase C and D, leading to intracellular calcium rise and eventual ROS production. The first-generation BTK inhibitor LFM-A13 reduced fMLF-induced calcium fluxes in neutrophils.<sup>43</sup> Using the same inhibitor, Gilbert et al.<sup>24</sup> observed reduced activation of PLD and the MAPK and Akt pathways in neutrophils, along with a decrease in Rac-2 recruitment to the membrane, which is an important cofactor for NADPH oxidase in ROS production. This was supported by data showing mild inhibition of fMLF-induced ROS production after *in vitro* pretreatment of human neutrophils with ibrutinib.<sup>37</sup> Additionally, neutrophils from chronic lymphocytic leukemia patients treated with ibrutinib exhibited a reduced oxidative burst and CXCL8 production upon *E. coli* stimulation.<sup>22</sup> Also, neutrophils from Btk-deficient mice displayed poor ROS production in response to LPS compared with wild-type mice.<sup>19</sup> Surprisingly, Honda et al.<sup>35</sup> reported BTK as a negative regulator of NADPH oxidase signaling, as excessive PMA-induced ROS production was found in neutrophils from X-linked agammaglobulinemia (XLA) patients characterized by BTK deficiency. Given that ROS production is essential for the release of NETs, specifically for DNA oxidation and subsequent chromatin decondensation,<sup>44</sup> we assessed NET production after treating neutrophils with BTK inhibitors. BTK inhibitor treatment reduced the release of NETs upon LPS stimulation. It has already been described that BTK is involved in TLR2/4 signaling by interacting with MyD88, MAL, and IRAK4 upstream of nuclear factor  $\kappa$ B activation.<sup>45,46</sup> Additionally, Risnik et al.<sup>37</sup> also reported impaired NET release after LPS stimulation in human neutrophils pretreated with ibrutinib. On the other hand, according to Marron et al.,<sup>47</sup> TLR signaling in neutrophils from XLA patients is unaffected compared with healthy donors. Intriguingly, when we exposed neutrophils to PGN, no clear effect of the compounds on NET release was observed. While inhibition of TLR4, the LPS receptor, was inadequate in preventing NET release, blocking ROS production in LPS-stimulated neutrophils completely abolished NET release.<sup>48</sup> This is in line with our results, as BTK was found to be indispensable for LPS-induced ROS production. In contrast, PGN activates TLR2 and the NOD-like receptor pathway in neutrophils. Activation of NOD1 and NOD2 (NLRC1/2) induces the autophagy pathway in immune cells by binding to RIP2. As BTK is not involved in this pathway, PGN responses can remain intact in the presence of BTK inhibitors.<sup>49</sup> PMA was used as positive control in our experiments as it penetrates neutrophils and directly activates PKC without receptor involvement. Activated PKC phosphorylates the cytosolic components of NADPH oxidase, leading to the assembly of the complex and enabling ROS production, without BTK involvement.<sup>50</sup>

We proceeded to investigate phagocytosis, using pH-sensitive bacterial bioparticles. Initially, we observed an increased fluorescent signal from engulfed particles after BTK inhibitor treatment. In contrast, the percentage of neutrophils that internalized a particle was not affected. Using sterile nanoparticles that were not pH

sensitive or TLR ligand coated, we confirmed that the phagocytosis machinery itself was not influenced by pretreating neutrophils with BTK inhibitors. After staining the cells with cresyl violet, a dye that exhibits increased fluorescence as the lysosomal pH decreases,<sup>33</sup> we demonstrated that BTK inhibitors influenced the lysosomal pH rather than the phagocytosis rate. Inhibition of BTK results in decreased ROS production by blocking the NADPH oxidase pathway. This enzyme typically consumes free protons to generate hydrogen peroxidase in the lysosome. BTK inhibitors inhibit this reaction, leading to an accumulation of intralysosomal protons and a subsequent drop in pH, compared with control neutrophils.<sup>51</sup>

To reach the site of infection or inflammation, neutrophils must extravasate from the blood circulation into surrounding tissues toward a chemoattractant. Although BTK inhibitors significantly reduced neutrophil migration toward both CXCL8 and fMLF in the Boyden chamber assay, tolebrutinib did not impact *in vivo* neutrophil chemotaxis toward CXCL1. Possible explanations include the need for adjustments in administration route or kinetics to ensure the drug reaches neutrophils at the right time. Moreover, conflicting literature on the murine BTK pathway and its compensatory mechanisms adds complexity, as other kinases of the TEC family might partially compensate for loss or inhibition of BTK activity in mice, which is not seen in humans.<sup>52,53</sup> Inconsistencies may also stem from the type of stimulus used. While Purvis et al.<sup>39</sup> reported a decrease in neutrophil attraction toward zymosan injection in ibrutinib-treated mice, no such effect was observed with CXCL1 as a chemoattractant.<sup>54</sup> Additionally, Volmering et al.<sup>40</sup> demonstrated that, in sterile inflammation, BTK is necessary for fMLF-induced MAC-1 activation and neutrophil recruitment. Bacterial products such as fMLF and LPS upregulate selectins on endothelial cells and ligands on neutrophils, leading to neutrophil rolling and activation of  $\beta$ 2-integrins (LFA-1 and MAC-1), in which BTK was recently proven to fulfill a crucial role.<sup>54</sup> These integrins can bind to intercellular adhesion molecules on the endothelium leading to cell arrest and diapedesis. Chemokines normally induce conformational activation of integrins in a G protein-coupled receptor-dependent manner, through signaling via RAP-1, where BTK is also believed to be involved.<sup>55</sup> However, some chemokines, including murine CXCL1, might activate alternative signaling pathways that rely on calcium influx through TRPC6, which is not described to be BTK dependent.<sup>56</sup> It is therefore possible that this pathway compensates for the reduced G protein-coupled receptor signaling in BTK inhibitor-treated mice. Despite the lack of an *in vivo* effect on CXCL1-induced chemotaxis, tolebrutinib still exhibited a strong inhibitory effect on ROS production in mouse bone marrow-derived neutrophils. Hence, it is still possible that intravenously injected tolebrutinib is captured by other factors or cells in the blood stream and is unable to affect circulating neutrophils. Therefore, we repeated the CXCL1 experiment but this time analyzed peritoneal leukocytes for their ability to produce ROS. Intriguingly, the peritoneally attracted neutrophils of the BTK inhibitor-treated animals showed reduced ROS production, compared with DMSO-treated mice. Thus, in mice, BTK inhibitors do not affect extravasation of neutrophils toward CXCL1, but rather reduce the ROS production by the attracted cells.

Finally, upon reaching the site of inflammation, neutrophils release cytokines and chemokines to attract other immune cells. To investigate the effect of BTK inhibitors on neutrophils' capacity to boost the inflammatory cascade by secreting CXCL8 or IL-1 $\beta$ , we quantified their release with ELISA after BTK inhibitor treatment. Here, we found that spontaneous CXCL8 production and

production of CXCL8 induced by fMLF, LPS, or IL-1 $\beta$  combined with TNF- $\alpha$  was significantly decreased after neutrophil pretreatment with all BTK inhibitors. Additionally, IL-1 $\beta$  production stimulated by LPS or IFN- $\gamma$  combined with TNF- $\alpha$  was reduced after neutrophil pretreatment with BTK inhibitors. This aligns with previous studies showing that LPS-induced production of TNF- $\alpha$  and IL-1 $\beta$  was blocked in neutrophils from Btk-deficient mice.<sup>57</sup> Moreover, it was demonstrated that BTK is involved in the inflammasome pathway resulting in active IL-1 $\beta$  release. Via physical interaction with NLRP3 and its adaptor protein ASC, BTK induces ASC oligomerization and caspase-1 activation.<sup>42</sup>

One limitation of our study is that the concentrations of BTK inhibitors used in most assays (micromolar range) may exceed the levels tested in patients during clinical trials. Indeed, IC<sub>50</sub> values of the 3 different BTK inhibitors used here are situated in the nanomolar range.<sup>58–60</sup> Still, peak serum concentrations reported in clinical trials approach the micromolar range (Supplementary Table 1). Overall, it remains a challenge to convert concentrations used in *in vitro* studies to *in vivo*, due to huge differences in environment and system. To exclude whether the drug effects on neutrophils reported here are related to a reduced selectivity at high concentrations, we performed dose-response experiments and found that BTK inhibitors still reduced cellular activation, ROS production, and NETs release at levels in the nanomolar range (Supplementary Fig. 10). However, we decided to go with the concentration from literature to ensure that the concentration was high enough to interfere with neutrophil effector mechanisms, as concentrations used in neutrophil studies are usually higher than those investigating B cell-mediated effects.<sup>58</sup>

Another limitation of this study relates to the fact that the 3 BTK inhibitors do not exclusively target BTK kinase. Due to conservation of the different characteristic enzyme domains within the TEC kinase family and high protein sequence similarity between BTK, BMX, and TEC kinase, it was up to now not possible to construct an inhibitor that selectively binds to BTK (Supplementary Table 1). More specifically, the crucial amino acid (C481) in the adenosine triphosphate binding pocket, which is targeted by irreversible BTK inhibitors, is also present in BMX and TEC, explaining the off-target binding to evobrutinib and tolebrutinib.<sup>61</sup> The noncovalent inhibitor fenebrutinib only targets BMX to a lesser extent, which most closely resembles BTK. It forms hydrogen bonds with K430, M477, and D539 residues, which are also found in BMX.<sup>62</sup> Our findings (Supplementary Fig. 11), along with data from the human genome atlas, demonstrate that expression of BTK in human mature neutrophils is the highest, followed by BMX and TEC kinase to a lesser extent. This suggests that the reported effects of BTK inhibitors may also partly reflect inhibition of BMX or TEC kinases. Despite the potential drawbacks of off-target binding, the simultaneous inhibition of BTK, BMX, and TEC kinases by BTK inhibitors could offer therapeutic opportunities. Indeed, BMX and TEC kinases have overlapping functions with BTK in several immune cell types and signaling pathways, and their inhibition could enhance the therapeutic effects of BTK inhibition in autoimmune disorders.

## 5. Conclusion

Taken together, our results show that pretreating human neutrophils *in vitro* with BTK inhibitors (evobrutinib, fenebrutinib, and tolebrutinib) reduces (1) neutrophil activation and actin polymerization by CXCL8 and fMLF, (2) migration toward CXCL8 and fMLF in a Boyden chamber, (3) ROS production, (4) NET release induced by LPS, (5) the intralysosomal pH, and (6) the production of CXCL8

and IL-1 $\beta$ . In contrast, tolebrutinib did not alter migration over a hCMEC/D3 monolayer, and *in vivo*, it did not reduce the migration of mouse neutrophils toward intraperitoneally injected CXCL1. However, the attracted peritoneal neutrophils are less capable of producing ROS. Considering these data, we recommend that neutrophil functionality should be monitored during follow-up of patients on BTK inhibitors, as it might affect patients' immune response toward concomitant infections. On the other hand, in light of the reported evidence of neutrophil involvement in pathogenic disease processes during MS, our work indicates that besides pathogenic B cells, specific neutrophil responses can also be dampened, revealing an additional mode of action of BTK inhibitors.

## Acknowledgments

The hCMEC/D3 cell line was provided by Tebu Bio. The authors thank all the healthy volunteers who donated blood for this research and Helga Ceunen, Stefanie Sente, and Shannon Nicolai for assistance in collecting blood samples.

## Author contributions

Investigation, data curation and analysis were performed by M.D.B., J.R., and P.P.d.P. Data curation and analysis was performed by N.B., M.G., L.V., and N.P. Conceptualization and methodology were developed by V.L.S.d.O., P.B., G.D., and B.B. Study conceptualization, project administration and supervision and editing/revising the manuscript were performed by P.M., N.H., and S.S. The original draft of the manuscript was written by M.D.B., and all authors commented on previous versions of the manuscript. All authors read and approved the final manuscript.

## Supplementary material

Supplementary material is available at *Journal of Leukocyte Biology* online.

## Funding

This work was financially supported by grants from the Research Foundation of Flanders, Bijzonder Onderzoeksfonds, UHasselt, KU Leuven, and the Belgian Charcot Foundation. M.D.B. and P.B. were financially supported by a personal grant from the Research Foundation of Flanders (1192221N and 1S87418N), G.D. by a grant from Bijzonder Onderzoeksfonds (BOF20DOC13), and M.G. by the Rega Foundation.

*Conflict of interest statement.* None declared.

## References

- Hauser SL, Cree BAC. Treatment of multiple sclerosis: a review. *Am J Med.* 2020;133(12):1380–1390.e2. <https://doi.org/10.1016/j.amjmed.2020.05.049>
- Walton C, King R, Rechtman L, Kaye W, Leray E, Marrie RA, Robertson N, La Rocca N, Uitdehaag B, van der Mei I, et al. Rising prevalence of multiple sclerosis worldwide: insights from the atlas of MS, third edition. *Mult Scler.* 2020;26(14):1816–1821. <https://doi.org/10.1177/1352458520970841>
- Filippi M, Bar-Or A, Piehl F, Preziosa P, Solari A, Vukusic S, Rocca MA. Multiple sclerosis. *Nat Rev Dis Primers.* 2018;4(1):43. <https://doi.org/10.1038/s41572-018-0041-4>

4. Reich DS, Lucchinetti CF, Calabresi PA. Multiple Sclerosis. *N Engl J Med*. 2018;378(2):169–180. <https://doi.org/10.1056/NEJMra1401483>
5. Bjornevik K, Cortese M, Healy BC, Kuhle J, Mina MJ, Leng Y, Elledge SJ, Niebuhr DW, Scher AI, Munger KL, et al. Longitudinal analysis reveals high prevalence of Epstein-Barr virus associated with multiple sclerosis. *Science*. 2022;375(6578):296–301. <https://doi.org/10.1126/science.abj8222>
6. Popescu BF, Pirko I, Lucchinetti CF. Pathology of multiple sclerosis: where do we stand? *Continuum (Minneapolis, Minn)*. 2013;19(4 Multiple Sclerosis):901–921. <https://doi.org/10.1212/01.CON.0000433291.23091.65>
7. Nylander A, Hafler DA. Multiple sclerosis. *J Clin Invest*. 2012;122(4):1180–1188. <https://doi.org/10.1172/JCI58649>
8. Aubé B, Lévesque SA, Paré A, Chamma É, Kébir H, Gorina R, Lécuyer M-A, Alvarez JI, De Koninck Y, Engelhardt B, et al. Neutrophils mediate blood-spinal cord barrier disruption in demyelinating neuroinflammatory diseases. *J Immunol*. 2014;193(5):2438–2454. <https://doi.org/10.4049/jimmunol.1400401>
9. Woodberry T, Bouffler SE, Wilson AS, Buckland RL, Brüstle A. The emerging role of neutrophil granulocytes in multiple sclerosis. *J Clin Med*. 2018;7(12):511. <https://doi.org/10.3390/jcm7120511>
10. Rosales C. Neutrophil: a cell with many roles in inflammation or several cell types? *Front Physiol*. 2018;9:113. <https://doi.org/10.3389/fphys.2018.00113>
11. De Bondt M, Hellings N, Opdenakker G, Struyf S. Neutrophils: underestimated players in the pathogenesis of multiple sclerosis (MS). *Int J Mol Sci*. 2020;21(12):4558. <https://doi.org/10.3390/ijms21124558>
12. Metzemaekers M, Malengier-Devlies B, Gouwy M, De Somer L, de Cunha FQ, Opdenakker G, Proost P. Fast and furious: the neutrophil and its armamentarium in health and disease. *Med Res Rev*. 2023;43(5):1537–1606. <https://doi.org/10.1002/med.21958>
13. Dolgin E. BTK blockers make headway in multiple sclerosis. *Nat Biotechnol*. 2021;39(1):3–5. <https://doi.org/10.1038/s41587-020-00790-7>
14. Lachance G, Levasseur S, Naccache PH. Chemotactic factor-induced recruitment and activation of tec family kinases in human neutrophils. Implication of phosphatidylinositol 3-kinases. *J Biol Chem*. 2002;277(24):21537–21541. <https://doi.org/10.1074/jbc.M201903200>
15. López-Herrera G, Vargas-Hernández A, González-Serrano ME, Berrón-Ruiz L, Rodríguez-Alba JC, Espinosa-Rosales F, Santos-Argumedo L. Bruton's tyrosine kinase—an integral protein of B cell development that also has an essential role in the innate immune system. *J Leukoc Biol*. 2014;95(2):243–250. <https://doi.org/10.1189/jlb.0513307>
16. Alu A, Lei H, Han X, Wei Y, Wei X. BTK inhibitors in the treatment of hematological malignancies and inflammatory diseases: mechanisms and clinical studies. *J Hematol Oncol*. 2022;15(1):138. <https://doi.org/10.1186/s13045-022-01353-w>
17. Martin E, Aigrot MS, Grenningloh R, Stankoff B, Lubetzki C, Boschert U, Zalc B. Bruton's tyrosine kinase inhibition promotes myelin repair. *Brain Plast*. 2020;5(2):123–133. <https://doi.org/10.3233/BPL-200100>
18. Reich DS, Arnold DL, Vermersch P, Bar-Or A, Fox RJ, Matta A, Turner T, Wallström E, Zhang X, Mareš M, et al. Safety and efficacy of tolebrutinib, an oral brain-penetrant BTK inhibitor, in relapsing multiple sclerosis: a phase 2b, randomised, double-blind, placebo-controlled trial. *Lancet Neurol*. 2021;20(9):729–738. [https://doi.org/10.1016/S1474-4422\(21\)00237-4](https://doi.org/10.1016/S1474-4422(21)00237-4)
19. Mangla A, Khare A, Vineeth V, Panday NN, Mukhopadhyay A, Ravindran B, Bal V, George A, Rath S. Pleiotropic consequences of Bruton tyrosine kinase deficiency in myeloid lineages lead to poor inflammatory responses. *Blood*. 2004;104(4):1191–1197. <https://doi.org/10.1182/blood-2004-01-0207>
20. Fiedler K, Sindrilaru A, Terszowski G, Kokai E, Feyerabend TB, Bullinger L, Rodewald HR, Brunner C. Neutrophil development and function critically depend on Bruton tyrosine kinase in a mouse model of X-linked agammaglobulinemia. *Blood*. 2011;117(4):1329–1339. <https://doi.org/10.1182/blood-2010-04-281170>
21. Broides A, Hadad N, Levy J, Levy R. The effects of Bruton tyrosine kinase inhibition on chemotaxis and superoxide generation in human neutrophils. *J Clin Immunol*. 2014;34(5):555–560. <https://doi.org/10.1007/s10875-014-0046-z>
22. Prezzo A, Cavaliere FM, Bilotta C, Pentimalli TM, Iacobini M, Cesini L, Foà R, Mauro FR, Quinti I. Ibrutinib-based therapy impaired neutrophils microbicidal activity in patients with chronic lymphocytic leukemia during the early phases of treatment. *Leuk Res*. 2019;87:106233. <https://doi.org/10.1016/j.leukres.2019.106233>
23. Blanter M, Cambier S, De Bondt M, Vanbrabant L, Pörtner N, Abouelasrar Salama S, Metzemaekers M, Marques PE, Struyf S, Proost P, et al. Method matters: effect of purification technology on neutrophil phenotype and function. *Front Immunol*. 2022;13:820058. <https://doi.org/10.3389/fimmu.2022.820058>
24. Gilbert C, Levasseur S, Desaulniers P, Dusseault AA, Thibault N, Bourgoin SG, Naccache PH. Chemotactic factor-induced recruitment and activation of Tec family kinases in human neutrophils. II. Effects of LFM-A13, a specific Btk inhibitor. *J Immunol*. 2003;170(10):5235–5243. <https://doi.org/10.4049/jimmunol.170.10.5235>
25. Guo R, Yan Z, Liao H, Guo D, Tao R, Yu X, Zhu Z, Guo W. Ibrutinib suppresses the activation of neutrophils and macrophages and exerts therapeutic effect on acute peritonitis induced by zymosan. *Int Immunopharmacol*. 2022;113:109469. <https://doi.org/10.1016/j.intimp.2022.109469>
26. Colado A, Marín Franco JL, Elías EE, Amondarain M, Vergara Rubio M, Sarapura Martínez V, Cordini G, Fuentes F, Balboa L, Fernandez Grecco H, et al. Second generation BTK inhibitors impair the anti-fungal response of macrophages and neutrophils. *Am J Hematol*. 2020;95(7):E174–E178. <https://doi.org/10.1002/ajh.25816>
27. Cockx M, Blanter M, Gouwy M, Ruytinx P, Abouelasrar Salama S, Knoops S, Pörtner N, Vanbrabant L, Lorent N, Boon M, et al. The antimicrobial activity of peripheral blood neutrophils is altered in patients with primary ciliary dyskinesia. *Int J Mol Sci*. 2021;22(12):12. <https://doi.org/10.3390/ijms22126172>
28. Proost P, Struyf S, Loos T, Gouwy M, Schutyser E, Conings R, Ronsse I, Parmentier M, Grillet B, Opdenakker G, et al. Coexpression and interaction of CXCL10 and CD26 in mesenchymal cells by synergising inflammatory cytokines: CXCL8 and CXCL10 are discriminative markers for autoimmune arthropathies. *Arthritis Res Ther*. 2006;8(4):R107. <https://doi.org/10.1186/ar1997>
29. Nguyen GT, Green ER, Meccas J. Neutrophils to the ROScUE: mechanisms of NADPH oxidase activation and bacterial resistance. *Front Cell Infect Microbiol*. 2017;7:373. <https://doi.org/10.3389/fcimb.2017.00373>
30. Mol S, Hafkamp FMJ, Varela L, Simkhada N, Taanman-Kueter EW, Tas SW, Wauben MHM, Groot Kormelink T, de Jong EC. Efficient neutrophil activation requires 2 simultaneous



- activating stimuli. *Int J Mol Sci*. 2021;22(18):10106. <https://doi.org/10.3390/ijms221810106>
31. Branzk N, Papayannopoulos V. Molecular mechanisms regulating NETosis in infection and disease. *Semin Immunopathol*. 2013;35(4):513–530. <https://doi.org/10.1007/s00281-013-0384-6>
32. Erbs G, Newman MA. The role of lipopolysaccharide and peptidoglycan, 2 glycosylated bacterial microbe-associated molecular patterns (MAMPs), in plant innate immunity. *Mol Plant Pathol*. 2012;13(1):95–104. <https://doi.org/10.1111/j.1364-3703.2011.00730.x>
33. Ostrowski PP, Fairn GD, Grinstead S, Johnson DE. Cresyl violet: a superior fluorescent lysosomal marker. *Traffic*. 2016;17(12):1313–1321. <https://doi.org/10.1111/tra.12447>
34. Kuhns DB, Young HA, Gallin EK, Gallin JI. Ca2+-dependent production and release of IL-8 in human neutrophils. *J Immunol*. 1998;161(8):4332–4339. <https://doi.org/10.4049/jimmunol.161.8.4332>
35. Honda F, Kano H, Kanegane H, Nonoyama S, Kim ES, Lee SK, Takagi M, Mizutani S, Morio T. The kinase Btk negatively regulates the production of reactive oxygen species and stimulation-induced apoptosis in human neutrophils. *Nat Immunol*. 2012;13(4):369–378. <https://doi.org/10.1038/ni.2234>
36. Krupa A, Fudala R, Florence JM, Tucker T, Allen TC, Standiford TJ, Luchowski R, Fol M, Rahman M, Gryczynski Z, et al. Bruton's tyrosine kinase mediates FcγRIIa/toll-like receptor-4 receptor cross-talk in human neutrophils. *Am J Respir Cell Mol Biol*. 2013;48(2):240–249. <https://doi.org/10.1165/rcmb.2012-0039OC>
37. Risnik D, Elías EE, Keitelman I, Colado A, Podaza E, Cordini G, Vergara Rubio M, Fernández Grecco H, Bezares RF, Borge M, et al. The effect of ibrutinib on neutrophil and γδ T cell functions. *Leuk Lymphoma*. 2020;61(10):2409–2418. <https://doi.org/10.1080/10428194.2020.1753043>
38. Nadeem A, Ahmad SF, Al-Harbi NO, Ibrahim KE, Alqahtani F, Alanazi WA, Mahmood HM, Alsanee S, Attia SM. Bruton's tyrosine kinase inhibition attenuates oxidative stress in systemic immune cells and renal compartment during sepsis-induced acute kidney injury in mice. *Int Immunopharmacol*. 2021;90:107123. <https://doi.org/10.1016/j.intimp.2020.107123>
39. Purvis GSD, Aranda-Tavio H, Channon KM, Greaves DR. Bruton's TK regulates myeloid cell recruitment during acute inflammation. *Br J Pharmacol*. 2022;179(11):2754–2770. <https://doi.org/10.1111/bph.15778>
40. Volmering S, Block H, Boras M, Lowell CA, Zarbock A. The neutrophil btk signalosome regulates integrin activation during sterile inflammation. *Immunity*. 2016;44(1):73–87. <https://doi.org/10.1016/j.immuni.2015.11.011>
41. Herter JM, Margraf A, Volmering S, Correia BE, Bradshaw JM, Bisconte A, Hill RJ, Langrish CL, Lowell CA, Zarbock A. PRN473, an inhibitor of Bruton's tyrosine kinase, inhibits neutrophil recruitment via inhibition of macrophage antigen-1 signalling. *Br J Pharmacol*. 2018;175(3):429–439. <https://doi.org/10.1111/bph.14090>
42. Ito M, Shichita T, Okada M, Komine R, Noguchi Y, Yoshimura A, Morita R. Bruton's tyrosine kinase is essential for NLRP3 inflammasome activation and contributes to ischaemic brain injury. *Nat Commun*. 2015;6(1):7360. <https://doi.org/10.1038/ncomms8360>
43. Zen K, Liu Y. Role of different protein tyrosine kinases in fMLP-induced neutrophil transmigration. *Immunobiology*. 2008;213(1):13–23. <https://doi.org/10.1016/j.imbio.2007.07.001>
44. Azzouz D, Khan MA, Palaniyar N. ROS induces NETosis by oxidizing DNA and initiating DNA repair. *Cell Death Discov*. 2021;7(1):113. <https://doi.org/10.1038/s41420-021-00491-3>
45. Jefferies CA, Doyle S, Brunner C, Dunne A, Brint E, Wietek C, Walch E, Wirth T, O'Neill LA. Bruton's tyrosine kinase is a toll/interleukin-1 receptor domain-binding protein that participates in nuclear factor kappaB activation by toll-like receptor 4. *J Biol Chem*. 2003;278(28):26258–26264. <https://doi.org/10.1074/jbc.M301484200>
46. Gray P, Dunne A, Brikos C, Jefferies CA, Doyle SL, O'Neill LA. Myd88 adapter-like (Mal) is phosphorylated by Bruton's tyrosine kinase during TLR2 and TLR4 signal transduction. *J Biol Chem*. 2006;281(15):10489–10495. <https://doi.org/10.1074/jbc.M508892200>
47. Marron TU, Rohr K, Martinez-Gallo M, Yu J, Cunningham-Rundles C. TLR signaling and effector functions are intact in XLA neutrophils. *Clin Immunol*. 2010;137(1):74–80. <https://doi.org/10.1016/j.clim.2010.06.011>
48. Pieterse E, Rother N, Yanginlar C, Hilbrands LB, van der Vlag J. Neutrophils discriminate between lipopolysaccharides of different bacterial sources and selectively release neutrophil extracellular traps. *Front Immunol*. 2016;7:484. <https://doi.org/10.3389/fimmu.2016.00484>
49. Moreira LO, Zamboni DS. NOD1 and NOD2 signaling in infection and inflammation. *Front Immunol*. 2012;3:328. <https://doi.org/10.3389/fimmu.2012.00328>
50. Damascena HL, Silveira WAA, Castro MS, Fontes W. Neutrophil activated by the famous and potent PMA (phorbol myristate acetate). *Cells*. 2022;11(18):2889. <https://doi.org/10.3390/cells11182889>
51. Westman J, Grinstead S. Determinants of phagosomal pH during host-pathogen interactions. *Front Cell Dev Biol*. 2021;8:624958. <https://doi.org/10.3389/fcell.2020.624958>
52. Ellmeier W, Jung S, Sunshine MJ, Hatam F, Xu Y, Baltimore D, Mano H, Littman DR. Severe B cell deficiency in mice lacking the tec kinase family members Tec and Btk. *J Exp Med*. 2000;192(11):1611–1624. <https://doi.org/10.1084/jem.192.11.1611>
53. de Bruijn MJ, Rip J, van der Ploeg EK, van Greuningen LW, Ta VT, Kil LP, Langerak AW, Rimmelzwaan GF, Ellmeier W, Hendriks RW, et al. Distinct and overlapping functions of TEC kinase and BTK in B cell receptor signaling. *J Immunol*. 2017;198(8):3058–3068. <https://doi.org/10.4049/jimmunol.1601285>
54. Mueller H, Stadtmann A, Van Aken H, Hirsch E, Wang D, Ley K, Zarbock A. Tyrosine kinase Btk regulates E-selectin-mediated integrin activation and neutrophil recruitment by controlling phospholipase C (PLC) gamma2 and PI3Kgamma pathways. *Blood*. 2010;115(15):3118–3127. <https://doi.org/10.1182/blood-2009-11-254185>
55. Polcik L, Dannewitz Prosseda S, Pozzo F, Zucchetto A, Gattei V, Hartmann TN. Integrin signaling shaping BTK-inhibitor resistance. *Cells*. 2022;11(14):2235. <https://doi.org/10.3390/cells1142235>
56. Lindemann O, Rossaint J, Najder K, Schimmelpfennig S, Hofschroer V, Walte M, Fels B, Oberleithner H, Zarbock A, Schwab A. Intravascular adhesion and recruitment of neutrophils in response to CXCL1 depends on their TRPC6 channels. *J Mol Med (Berl)*. 2020;98(3):349–360. <https://doi.org/10.1007/s00109-020-01872-4>
57. Uckun FM, Qazi S. Bruton's tyrosine kinase as a molecular target in treatment of leukemias and lymphomas as well as inflammatory disorders and autoimmunity. *Expert Opin Ther Pat*. 2010;20(11):1457–1470. <https://doi.org/10.1517/13543776.2010.517750>
58. Haselmayer P, Camps M, Liu-Bujalski L, Nguyen N, Morandi F, Head J, O'Mahony A, Zimmerli SC, Bruns L, Bender AT, et al. Efficacy and pharmacodynamic modeling of the BTK inhibitor

- evobrutinib in autoimmune disease models. *J Immunol*. 2019;202(10):2888–2906. <https://doi.org/10.4049/jimmunol.1800583>
59. Dahl K, Turner T, Vasdev N. Radiosynthesis of a Bruton's tyrosine kinase inhibitor, [<sup>11</sup>C]tolebrutinib, via palladium-NiXantphos-mediated carbonylation. *J Labelled Comp Radiopharm*. 2020;63(11):482–487. <https://doi.org/10.1002/jlcr.3872>
60. Herman AE, Chinn LW, Kotwal SG, Murray ER, Zhao R, Florero M, Lin A, Moein A, Wang R, Bremer M, et al. Safety, pharmacokinetics, and pharmacodynamics in healthy volunteers treated with GDC-0853, a selective reversible Bruton's tyrosine kinase inhibitor. *Clin Pharmacol Ther*. 2018;103(6):1020–1028. <https://doi.org/10.1002/cpt.1056>
61. Smith CIE, Islam TC, Mattsson PT, Mohamed AJ, Nore BF, Vihinen M. The Tec family of cytoplasmic tyrosine kinases: mammalian Btk, Bmx, Itk, Tec, Txk and homologs in other species. *Bioessays*. 2001;23(5):436–446. <https://doi.org/10.1002/bies.1062>
62. Crawford JJ, Johnson AR, Misner DL, Belmont LD, Castaneda G, Choy R, Coraggio M, Dong L, Eigenbrot C, Erickson R, et al. Discovery of GDC-0853: a potent, selective, and noncovalent Bruton's tyrosine kinase inhibitor in early clinical development. *J Med Chem*. 2018;61(6):2227–2245. <https://doi.org/10.1021/acs.jmedchem.7b01712>